Pergamon

Geochimica et Cosmochimica Acta, Vol. 68, No. 4, pp. 841–865, 2004

0016-7037/04 $30.00 + .00

doi:10.1016/j.gca.2003.07.009

Volcanic arc of Kamchatka: a province with high-$\delta^{18}O$ magma sources and large-scale $^{18}O/^{16}O$ depletion of the upper crust

ILYA N. BINDEMAN,[1,*] VERA V. PONOMAREVA,[2] JOHN C. BAILEY,[3] and JOHN W. VALLEY[1]

[1]Department of Geology and Geophysics, University of Wisconsin, Madison, WI, USA
[2]Institute of Volcanic Geology and Geochemistry, Petropavlovsk-Kamchatsky, Russia
[3]Geologisk Institut, University of Copenhagen, Copenhagen, Denmark

(*Received March* 20, 2003; *accepted in revised form July* 16, 2003)

Abstract—We present the results of a regional study of oxygen and Sr-Nd-Pb isotopes of Pleistocene to Recent arc volcanism in the Kamchatka Peninsula and the Kuriles, with emphasis on the largest caldera-forming centers. The $\delta^{18}O$ values of phenocrysts, in combination with numerical crystallization modeling (MELTS) and experimental fractionation factors, are used to derive best estimates of primary values for $\delta^{18}O$(magma). Magmatic $\delta^{18}O$ values span 3.5‰ and are correlated with whole-rock Sr-Nd-Pb isotopes and major elements. Our data show that Kamchatka is a region of isotopic diversity with high-$\delta^{18}O$ basaltic magmas (sampling mantle to lower crustal high-$\delta^{18}O$ sources), and low-$\delta^{18}O$ silicic volcanism (sampling low-$\delta^{18}O$ upper crust). Among one hundred Holocene and Late Pleistocene eruptive units from 23 volcanic centers, one half represents low-$\delta^{18}O$ magmas (+4 to 5‰). Most low-$\delta^{18}O$ magmas are voluminous silicic ignimbrites related to large >10 km^3 caldera-forming eruptions and subsequent intracaldera lavas and domes: Holocene multi-caldera Ksudach volcano, Karymsky and Kurile Lake-Iliinsky calderas, and Late Pleistocene Maly Semyachik, Akademy Nauk, and Uzon calderas. Low-$\delta^{18}O$ magmas are not found among the less voluminous products of stratovolcano eruptions and these volcanoes do not show drastic changes in $\delta^{18}O$ during their evolution. Additionally, high-$\delta^{18}O$(magma) of +6.0 to 7.5‰ are found among basalts and basaltic andesites of Bezymianny, Shiveluch, Avachinsky, and Koryaksky volcanoes, and dacites and rhyolites of Opala and Khangar volcanoes (7.1–8.0‰). Phenocrysts in volcanic rocks from the adjacent Kurile Islands (ignimbrites and lavas) define normal-$\delta^{18}O$ magmas. The widespread and volumetric abundance of low-$\delta^{18}O$ magmas in the large landmass of Kamchatka is possibly related to a combination of near-surface volcanic processes, the effects of the last glaciation on high-latitude meteoric waters, and extensive geyser and hydrothermal systems that are matched only by Iceland. Sr and Pb isotopic compositions of normal and low-$\delta^{18}O$, predominantly silicic, volcanic rocks show negative correlation with $\delta^{18}O$, similar to the trend in Iceland. This indicates that low-$\delta^{18}O$ volcanic rocks are largely produced by remelting of older, more radiogenic, hydrothermally altered crust that suffered $\delta^{18}O$-depletion during >2 My-long Pleistocene glaciation. The regionally-distributed high-$\delta^{18}O$ values for basic volcanism (ca. + 6 to +7.5‰) in Kamchatka cannot be solely explained by high-$\delta^{18}O$ slab fluid or melt (± sediment) addition in the mantle, or local subduction of hydrated OIB-type crust of the Hawaii-Emperor chain. Overall, Nd-Pb isotope systematics are MORB-like. Voluminous basic volcanism (in the Central Kamchatka Depression in particular) requires regional, though perhaps patchy, remobilization of thick (30–45 km) Mesozoic-Miocene arc roots, possibly resulting from interaction with hot (ca. 1300°C), wedge-derived normal-$\delta^{18}O$, low-$^{87}Sr/^{86}Sr$ basalts and from dehydration melting of lower crustal metabasalts, variably high in $\delta^{18}O$ and $^{87}Sr/^{86}Sr$. *Copyright © 2004 Elsevier Ltd*

1. INTRODUCTION

Dynamic interplay between glaciations and volcanic activity is seen during the Pleistocene history of the northern circum-Pacific region. Voluminous caldera-forming eruptions, glacial advances, and rapid sea level changes, have affected local and global climate; recent studies recognize the importance of the North Pacific in paleoclimate reconstruction (e.g., Bradley, 2000; Gualtieri et al., 2001; Beget, 2001; Brigham-Grette, 2001). Glaciation may have local and regional effects on volcanism; rapid pressure release during deglaciation may help trigger eruptions (e.g., Nakada and Yokose, 1992), but the broader effects are poorly understood. Many ash layers and H_2SO_4-rich horizons in the Pleistocene-Holocene Greenland ice core record are now attributed to sources in Kamchatka and the Aleutian island arc (e.g., Zielinski et al., 1996; Braitseva et al., 1997b). The Kamchatka Peninsula overlies the northwestern margin of the subducting Pacific plate and is one of the most volcanically active area in the Holocene (Simkin and Siebert, 1994), and probably has the largest exposed hydrothermal and geyser system at high latitudes.

This paper was prompted by the discovery that Kamchatka is a land of isotopic diversity with high-$\delta^{18}O$ basic magmas and low-$\delta^{18}O$ upper crust. Low-$\delta^{18}O$ magmas are here defined as <5.5‰ for basalts to < 5.8‰ for rhyolites; high-$\delta^{18}O$ magmas are >6.0‰ for basalts, and >6.4‰ for rhyolites, see section 4.1 below. Evidence is presented that Kamchatka is a high-latitude volcanic province with an abundance of low-$\delta^{18}O$ rocks (based on number of low-$\delta^{18}O$ units and their total volume) matched only by Iceland. We attribute this to the effect of Pleistocene glaciation on meteoric waters, hydrothermally-

* Author to whom correspondence should be addressed, at Division of Geological and Planetary Sciences, California Institute of Technology, Pasadena, CA 91125, USA (inbindem@gps.caltech.edu).

altered rocks, and magmas (cf. Donnely-Nolan, 1998; Gautason and Muehlenbachs, 1998; Bindeman et al., 2001).

No low-δ^{18}O magmas have been found in low-latitude arcs of the circum-Pacific, or other island arcs, but normal- and high-δ^{18}O magmas are common (Taylor, 1968; Matsuhisa, 1979; Macpherson et al., 1998; Vroon et al., 2001). At high-latitudes, the Fisher and Okmok calderas (Aleutians) produced low-δ^{18}O magmas (Bindeman et al., 2001), and more low-δ^{18}O magmas are likely to be found there: like Kamchatka, the Aleutian arc is a volcanically active subpolar area that underwent Pleistocene glaciation.

This study uses the *primary* range of magmatic δ^{18}O values in Kamchatkan magmas based on analyses of phenocrysts in combination with the radiogenic isotopes of Sr, Nd, and Pb determined on whole rocks to provide key constraints on the genesis of both high- and low-δ^{18}O magmas discovered in Kamchatka. Such an approach is used to define the role of deep (slab and mantle) processes vs. shallow processes of crustal recycling, and was used in the past to describe more subdued δ^{18}O ranges in other island arcs and other settings (e.g., Thirlwall et al., 1996; Baker et al., 2000; Eiler et al., 2000a,b; Vroon et al., 2001). We here present evidence that lower and upper crustal processes dominate the petrogenesis of basic and silicic magmas in Kamchatka, though a mantle signature can still be recognized in some trace elements and isotopes.

2. KAMCHATKAN VOLCANISM

2.1. Eruptive Centers, Volcanic Rocks, and ^{14}C-Dated Tephra Layers

The Kamchatka volcanic belt is a part of the Kurile-Kamchatka volcanic arc related to the subduction of the Pacific plate (Fig. 1). Eruptive centers differ in their tectonic position relative to the present volcanic front and can be grouped into three tectonic zones (Fig. 1): Eastern Volcanic Front (EVF), Central Kamchatka Depression (CKD), and Sredinny Range (SR). Magmatic volumes generally decrease westward, but Recent volcanism is most voluminous in the CKD with some of the largest volcanoes of the world such as Klyuchevskoy. Volcanic rocks of the Kurile-Kamchatka island arc span compositions from basalt to rhyolite, from tholeiitic to calc-alkaline, and from low- to high-K and shoshonitic series (Fig. 2; Volynets, 1994; Bailey, 1996). Olivine-phyric basalts are relatively rare, and typical silicic rocks tend to lack quartz and zircon. The majority of rocks are either basaltic andesites or andesites. This is a common feature of island arcs, and regional oxygen isotope studies must rely primarily on the analyses of ubiquitous plagioclase, pyroxene, and amphibole phenocrysts.

Unlike many previous studies, we emphasize the importance of dated tephra and ignimbrites from products of major caldera-forming eruptions ranging from Pleistocene to Holocene and studied in detail during the last decade (Braitseva and Melekestsev, 1990; Braitseva et al., 1995, 1996, 1997a,b; Leonov and Grib, 1998; Volynets et al., 1999; Ponomareva et al., 2004). The ^{14}C-dated Holocene tephras analyzed in this study (Table A1, Electronic Annex, Elsevier Website, Science Direct) are preserved regionally; they provide an important record of voluminous eruptions and serve as tephrochronological markers (Braitseva et al., 1995, 1997a). Identified regional tephras create a framework of Holocene volcanic activity, which is pertinent to volcanology, dating marine sediments (Prueher and Rea, 2001a), impact on climate (Braitseva et al., 1997b; Prueher and Rea, 2001b), and archeology (Braitseva et al., 1987). Pleistocene and older ignimbrite and tephra layers are unambiguously found in the vicinity of large calderas ($>$10 km in diameter): Pauzhetka, Uzon, Maly Semyachik, Akademy Nauk, and others (e.g., Grib and Leonov, 1993a,b). Most tephras at each eruptive center represent differentiated products, typically silicic andesite to rhyolite, occurring in caldera settings, and are distinct mineralogically and chemically. Given the predominantly NE direction of winds, tephra layers from major eruptions have been deposited in the Beringia Terrain (Fig. 1, inset), and numerous layers of abundant Kamchatkan volcanic ash are identified in ODP marine sediments in the NW Pacific (Bailey, 1993, 1996; Prueher and Rea, 2001a,b).

2.2. Glaciations

Kamchatka experienced several voluminous glaciations during Pleistocene (Braitseva et al., 1968; Grosswald, 1998). Ice covered most volcanic edifices even in southern Kamchatka (Melekestsev et al., 1974; Savoskul, 1999). Starting from the beginning of glaciation at 2.6 Ma, ice repeatedly reached seashores and supplied debris and iceberg-rafted material to marine sediments (Prueher and Rea, 2001b). At present, the snow line is at $\sim$1000m elevation, and many volcanic edifices contain patchy glaciers.

2.3. Previous Stable Isotope Studies

Phenocryst-based oxygen isotope studies in Kamchatka have been limited; most reported analyses are for whole-rocks that are prone to postmagmatic alteration, and concentrated on the petrogenesis of basalts. Pokrovsky and Volynets (1999) and Pineau et al. (1999) demonstrated a moderate ($\sim$1‰) increase in whole-rock δ^{18}O values across the arc. Dorendorf et al. (2000) discovered that olivines and pyroxenes from Klyuchevskoy volcano have high-δ^{18}O values (6–7.5‰) and attributed this to the addition of high-δ^{18}O slab fluids to the mantle generation zones. In the study of differentiated products, Pokrovsky and Volynets (1999) noted that many ignimbrites in Kamchatka are characterized by ^{18}O-depleted whole-rock values, which result from secondary hydrothermal alteration or magmatic assimilation of hydrothermally-altered rocks. We have compiled published whole-rock δ^{18}O values for Kamchatka and plotted them vs. ^{87}Sr/^{86}Sr for the same volcanic units (Fig. 3A). The δ^{18}O values for basalts and basaltic andesites, based on the petrographically freshest and least hydrated ($<$1.1wt% H_2O) whole-rock analyses, span the range from 5.4 to 8.5‰, and 0.703 to 0.706 for ^{87}Sr/^{86}Sr (Ivanov, 1990; Pineau et al., 1999; Pokrovsky and Volynets, 1999). Strontium and oxygen isotope studies of the exposed outcrops of Cretaceous to Miocene metamorphic basements (Fig. 3B) demonstrate positive correlation, with higher ^{87}Sr/^{86}Sr and δ^{18}O values for silicic metamorphic rocks of the Sredinny Massif (SM, see Fig. 1). Geothermal waters in Kamchatka (Vinogradov and Vakin, 1983; Taran et al., 1988; Chesho, 1994) are low in δ^{18}O and δD, and seems to inherit these relatively high ^{87}Sr/^{86}Sr values, even for geothermal systems

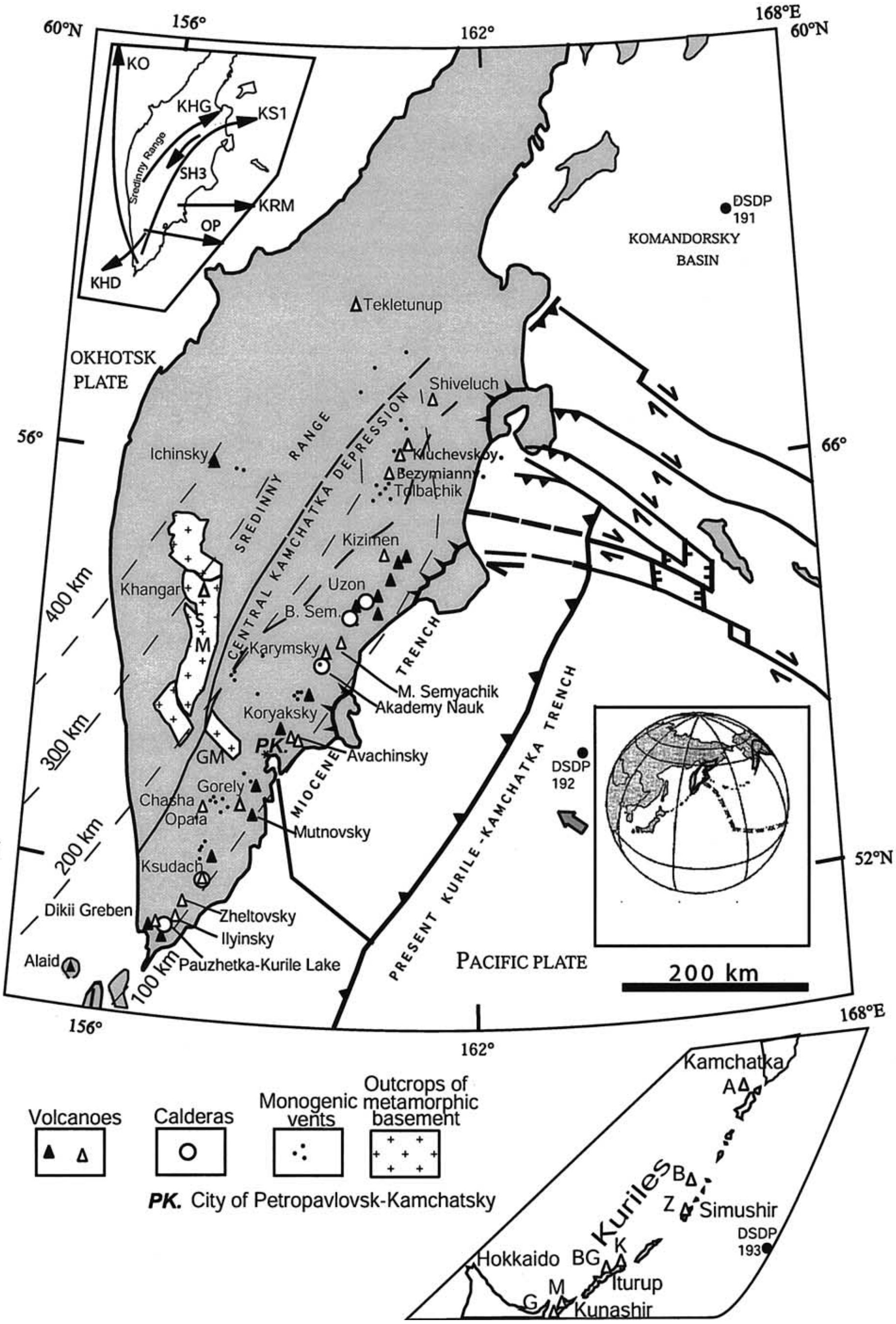

Fig. 1. Map of Kamchatka Peninsula showing Holocene volcanic centers, major Holocene and Late Pleistocene calderas, and regional geodynamic features after Bogdanov and Khain (2000) and Baranov (1991). The upper inset shows the direction of tephra deposition (Braitseva et al., 1997a) for most voluminous Holocene eruptions; tephra codes are from Table A1 (Electronic Annex). Lower inset shows global position of Kurile-Kamchatka arc and interconnected glacial covers from Mann and Peteet (1994) and Braitseva et al. (1968). Selected calderas and volcanoes of the Kurile island arc analyzed in this study (Table 1; and Table A1, Electronic Annex) are shown in the lower figure. G = Golovnin caldera; M = Mendeleyev volcano; BG = Bogdan Khmelnitsky volcano; K = Kudriavy volcano; Z = Zavaritsky caldera; B = Brouton volcano; A = Alaid volcano. Open triangles and circles are studied volcanoes and calderas. Volcanism in Kamchatka occurs in three structural zones: the Eastern Volcanic Front (EVF), the Central Kamchatka Depression (CKD), and the Sredinny Range (SR). Following Late Miocene accretion of the Eastern Peninsula Terrains (Geist et al., 1994), the subduction trench rolled back 200 km to the east to its present position (Volynets, 1994) and the present position of the Kurile-Kamchatka volcanic front was established. Presently active volcanoes (Khangar, Ichinsky) are located on the Cretaceous to Eocene siliceous metamorphic basement (Sredinny Massif, SM). To the east, mafic crust is exposed as high-grade metamorphic rocks of Ganal Massif (GM) of Cretaceous to Miocene age. Petrology, ages, and tectonic mechanisms of accretion are discussed in Geist et al. (1994); Tatsumi et al. (1995); Konstantinovskaya (2000); Bogdanov and Khain (2000) and Bindeman et al. (2002).

Fig. 1. (Continued) Thus, recent volcanism is built upon a series of Mesozoic terranes with both felsic (SR) and mafic crusts (EVF, CKD,) with low $^{87}Sr/^{86}Sr$ (0.703 to 0.706, Vinogradov, 1995) that form 30 to 45 km thick crust (Bogdanov and Khain, 2000). In the NW Pacific and Kamchatka, nearly orthogonal subduction, dipping at ~45° angle of the Cretaceous Pacific plate for the past 43 Ma (e.g., Engebretson et al., 1985; Nokleberg et al., 1998) has enriched the mantle wedge with volatiles and, as is discussed in the text, has caused a regionally extensive high $\delta^{18}O$ source. Accreted oceanic arcs have added high-$\delta^{18}O$ mafic and silicic rocks (Fig. 3B) to the lower crust/mantle.

far from the surface outcrops of metamorphic basements; this causes elevation of $^{87}Sr/^{86}Sr$ in ^{18}O-depleted hydrothermally-altered rocks (Fig. 3B). Values of $\delta^{18}O$ and δD of fumarolic gases (Taran et al., 1988, 1997) indicate a significant proportion of meteoric water.

2.4. Radiogenic Isotope Studies

Sr, Nd, Pb, Th, Os, Be, and B isotopic, as well as trace elemental studies have been performed on Kamchatkan and Kurile volcanoes, and sediments in the NW Pacific, and correlated to tectonic position and depth to the Benioff zone (Bailey et al., 1987; Zhuravlev et al., 1987; Tera et al., 1990; Bailey, 1993, 1996; Kersting and Arculus, 1994, 1995; Volynets, 1994; Hochstaedter et al., 1996; Leeman, 1996; Kepezhinskas et al., 1997; Plank and Langmuir, 1998; Turner et al., 1998; Dorendorf et al., 2000; Ishikawa et al., 2001; Widom et al., 2003). Most of radiogenic isotope variations are interpreted to indicate that: 1) isotopic compositions of primary Kamchatkan lavas are primitive and similar to Pacific MORB; 2) there is a small amount of sediment input into magma generation zones; 3) there are across-arc and along-arc variations in isotopic parameters and in Ce/Y, Ba/Th, La/Ta, B/Nb suggesting differences in fluid release as a function of slab depth (e.g., Ishikawa et al., 2001); 4) most samples plot near the equiline on the $^{230}Th/^{232}Th$ vs. $^{238}U/^{232}Th$ diagram pointing that >150 k.y. has elapsed since fluid release from the slab and eruption of magmas (e.g., Turner et al., 1998); however voluminous basic rocks from the Central Kamchatka Depression show larger disequilibria and may require "shorter" timescales (Dosseto and Bourdon, 2002); and 5) $^{10}Be/^{9}Be$ in Kamchatka are lower than in the Aleutians or the Kuriles (e.g., Tera et al., 1990; Ryan et al., 1995) suggesting longer magma residence times and/or derivation of magma from different mantle and crustal sources.

Whereas mantle- and slab-derived processes are currently interpreted to be the dominant control on radiogenic isotope systematics of Kamchatkan magmas, as in the Kuriles and Aleutians, the Kamchatkan volcanism has some additional features. Voluminous volcanism, some with adakitic (high Sr/Y) affinities (Drummond et al., 1996) in the CKD is attributed to melting of the Pacific slab due to mantle corner flow around the plate edge (Yogodzinski et al., 2001). Neogene subduction of the Meiji and Emperor Seamount Chain may cause an alkaline imprint and high magma production rates in Klyuchevskoy and other volcanoes of CKD (Kersting and Arculus, 1994, 1995; Bailey, 1996). These features are shown to be more regional by recent mantle tomography (Gorbatov et al., 2001); a wide ocean-ward mantle plume with anomalous high heat flow heats and thins the oceanic lithosphere before it is subducted under

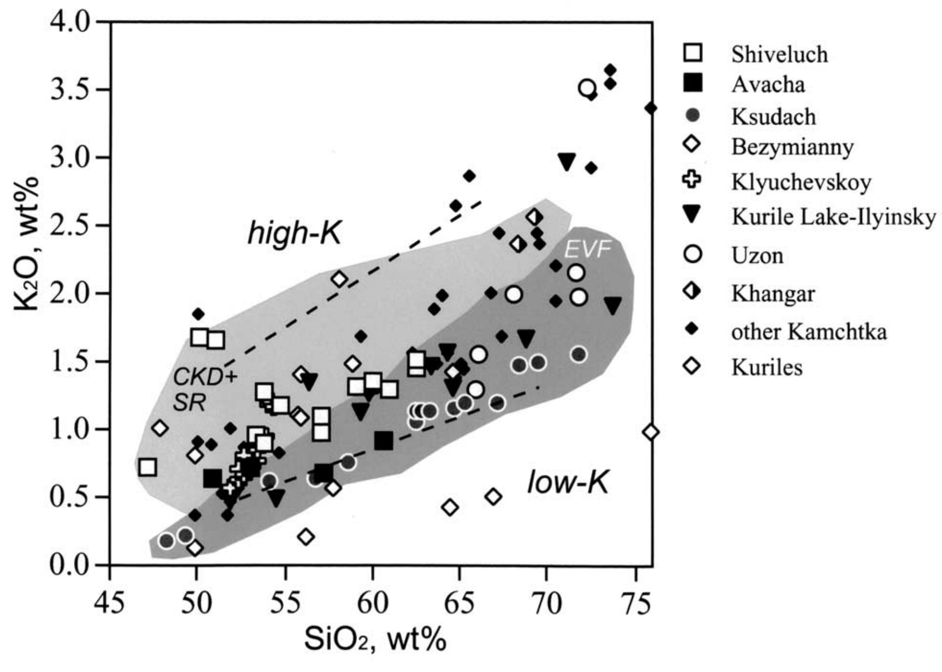

Fig. 2. Major element composition of samples analyzed in this study K_2O vs. SiO_2. See Table A1 (Electronic Annex) for analyses. Dashed lines divides low-, medium-, and high-K volcanic arc series (Gill, 1981). CKD and SR lavas tend to be more K-rich than EVF lavas. Klyuchevskoy data are from Dorendorf et al. (2000).

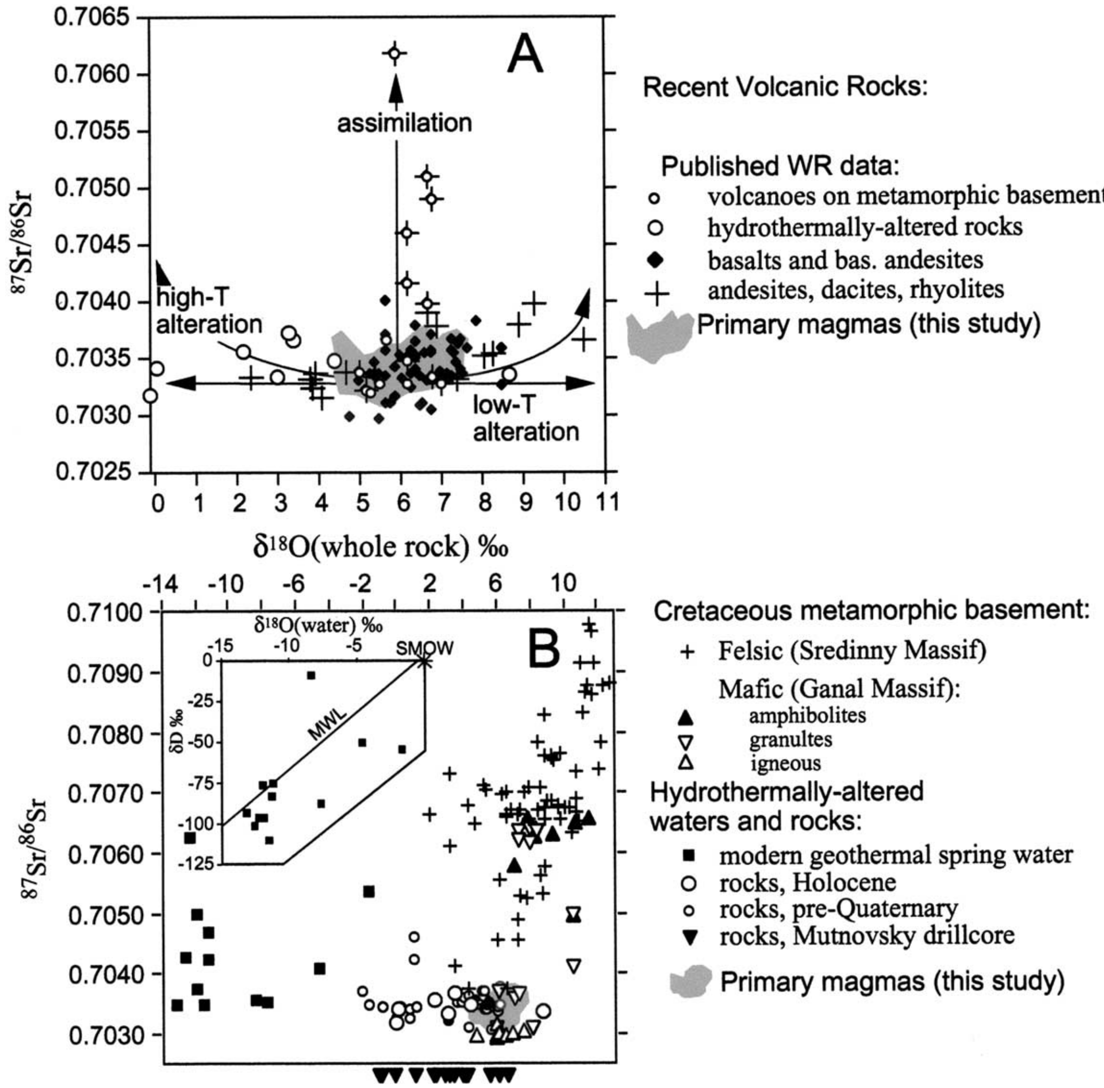

Fig. 3. Correlation of $\delta^{18}O$(whole rock) vs. $^{87}Sr/^{86}Sr$. (A) Quaternary Kamchatkan volcanic rocks. Published $\delta^{18}O$(whole rock) analyses indicate that shallow processes of isotopic exchange and alteration dominate over primary (source) characteristics. Whole-rock data from published sources indicate wide ranges due to high- and low-temperature exchange with meteoric waters, which affect $\delta^{18}O$(whole rock) much more than $^{87}Sr/^{86}Sr$ ratios. In contrast, assimilation of older metamorphic Mesozoic crust of Sredinny Range preferentially changes $^{87}Sr/^{86}Sr$ (highest $^{87}Sr/^{86}Sr$ values are from lower Pleistocene Belogolovsky volcano on SR, Pokrovsky and Volynets, 1999). (B) $\delta^{18}O$(whole rock) vs. $^{87}Sr/^{86}Sr$ in other crustal materials: mafic (Ganal terrane) and felsic (Sredinny Range) metamorphic rocks from the basement, hydrothermally altered rocks, and geothermal waters of modern hydrothermal systems. Inset shows δD vs. $\delta^{18}O$ in hydrothermal (100–300°C) waters (Vinogradov and Vakin, 1983) relative to present-day meteoric water line (MWL). Isotope data are compiled from Taran et al. (1988), Ivanov (1990), Volynets (1994), Vinogradov (1995), Zolotarev et al. (1999), Pokrovsky and Volynets (1999), and Dril et al. (1999).

Kamchatka. Additionally, slab detachments at 10 and 2 Ma (Levin et al., 2003) may have contributed to the diffuse monogenetic magmatism with intraplate geochemical affinity that occurs predominantly in the back arc (Volynets, 1994). All these mantle-derived magmas rise through thick 30–45 km continental crust that exists beneath Kamchatka (Bogdanov and Khain, 2000).

These observations suggest that Kamchatka is a geochemically complex arc system where mantle-derived magmatism is tectonically diverse and driven by a variety of processes. In contrast to previous studies and interpretations, this paper demonstrates a largely crustal origin for most silicic and some basic magmatism, as has long been advocated in other island arc systems (e.g., Davidson, 1989). It indicates the importance of recycling of older arc volcanic material in Recent volcanism, and indirect influence of last glaciation on the isotopic signatures of magmatism.

3. ANALYTICAL TECHNIQUES

We analyzed phenocrysts by laser fluorination to determine primary magmatic $\delta^{18}O$ values at the University of Wisconsin. Phenocrysts are shown to be unaltered by petrographic inspection, and by analysis of at least two minerals in a rock, by duplicate analyses of individual (1–2 mg) phenocrysts (e.g., plagioclase), and calculation of magmatic mineral-mineral fractionations. Analyses of plagioclase, olivine, clinopyroxene, amphibole, and quartz phenocrysts allow derivation of magmatic values using experimental and empirical mineral-melt and mineral-mineral isotopic fractionations (see below and Appendix). Several petrographically fresh whole-rock powders for which mineral separates were unavailable were analyzed; their magmatic $\delta^{18}O$ values are treated with caution. Analyzed mineral aliquots were typically 1–2 mg, yielding 10–30 μmol of CO_2; yields were 90–102%, and there is no correlation between yield, sample size, and $\delta^{18}O$. Minerals were pretreated with 5 torr of BrF_5 overnight to remove any surface or water contamination. The CO_2 laser fluorination lab yielded precise ($\pm$ 0.1‰, 1 st dev) analyses, used BrF_5 reagent, and conversion to CO_2 gas following fluorination. Four to nine UWG-2 garnet standards (+5.8‰, corresponding to NBS28 = 9.6‰, Valley et al., 1995) were analyzed during each analytical session, and yielded 5.75 $\pm$ 0.10‰ (1 st dev). Eleven NBS-28 quartz standards yielded a value of +9.46 $\pm$ 0.08‰ (1 st dev). Whole rock powders (~2 mg) were analyzed one at a time using an airlock chamber. A correction in the range of +0.3‰ to −0.05‰ (+0.15 to 0‰ for most days) was applied to account for day-to-day variations based on values of 5 to 7 UWG-2 garnets measured during each analytical session. Thus, the overall analytical uncertainty on single measurements is better than $\pm$ 0.10‰ (1 st dev).

Sr, Nd, and Pb isotopes were analyzed in the University of Copenhagen by TIMS (VG Sector 54-IT) using standard preparation techniques of acid digestion (HBr, HNO_3, and HF) and cation-exchange chromatography. Sr-isotopic ratios were measured in the dynamic mode; Rb interferences were corrected for mass fractionation to $^{87}Sr/^{86}Sr$ = 0.1194. Reproducibility was tested by measuring standard NBS987 which yielded $^{87}Sr/^{86}Sr$ = 0.710244 $\pm$ 13 (1 st dev). Nd isotope ratios were corrected for Sm interference and for mass fractionation $^{146}Nd/^{144}Nd$ = 0.7219. The laboratory JM Nd standard gave $^{144}Nd/^{144}Nd$ = 0.511108 $\pm$ 13 (1 st dev). Pb isotopic composition was fractionation-corrected on average by 0.12% per a.m.u., relative to Pb standard NBS981; repeated analyses of this standard yielded $^{206}Pb/^{204}Pb$ = 16.890–16.895 in the course of this work. Selected samples were also analyzed for major and trace elements (Table A1, Electronic Annex) by XRF (Philips PW1400) at the Geological Institute of the University of Copenhagen.

4. DIFFERENTIATION MODELING

4.1. Normal-δ^{18}O, Low-δ^{18}O, and High-δ^{18}O Magmas

In this work we define normal-$\delta^{18}O$ magmas as having an oxygen isotope ratio consistent with derivation by crystal differentiation from basalt of an arc-mantle source (+5.8 $\pm$ 0.2‰). Since the present work considers rocks of different SiO_2 content, it is important to estimate how much $\delta^{18}O$ variation can be attributed to fractional crystallization. There have been a number of attempts in the past to estimate and parameterize $\delta^{18}O$ change with compositional differentiation monitors, such as SiO_2, MgO and Fe/Mg used to measure increasing differentiation (e.g., Taylor, 1968; Anderson et al., 1971; Matsuhisa et al., 1973; Matsuhisa, 1979; Muehlenbachs and Byerly, 1982; Kalamarides, 1984; Eiler, 2001). There is an overall agreement that differentiation from basalt to rhyolite produces a positive subper mil change in $\delta^{18}O$ melt, since the bulk cumulate has variable but lower $\delta^{18}O$ than the residual melt. However, there are disagreements on the absolute range (from 0 to >1‰) and trajectory of $\delta^{18}O$(melt) change with SiO_2.

The modeling of $\delta^{18}O$ shift due to fractional crystallization is becoming increasingly important since the improved analytical precision of oxygen isotope analysis (better than $\pm$ 0.05–0.1‰), can now resolve the cause for small (ca. <0.5‰) variations, whether due to differentiation, partial melting of the same homogeneous mantle reservoir at different P-T-X_{H2O} conditions, or interaction with other reservoirs. This has particular relevance for volcanic arcs where the magmatic rocks are characterized by a significant range of SiO_2 contents, and a number of variable $\delta^{18}O$ reservoirs (slab, mantle wedge, crust, or fluids) are thought to contribute to petrogenesis.

In this work, we undertook modeling (MELTS) of fractional crystallization of several typical arc basaltic compositions of Kamchatka (high-Mg, high-Al, high-alkali, Table A2, Electronic Annex) to derive the magnitude and trajectory of $\delta^{18}O$ increase with differentiation as a function of pressure and water content. We have attempted similar crystallization modeling with Kurile Island arc compositions in the past (Bindeman and Bailey, 1999); this yielded results in agreement with the observed chemical compositions of melts and minerals (plagioclase in particular).

Knowledge of melting relations and $^{18}O/^{16}O$ isotopic fractionations guided the choice of initial compositions and experimental parameters to derive the most 'extreme' (or end-member-case) isotopic effects. In particular, low pressures and more oxidizing conditions promote early crystallization of olivine and magnetite, minerals that have the most negative $\Delta^{18}O$(mineral-melt), and promote the largest increase in $\delta^{18}O$(melt). Higher water pressures enhance the crystallization fields of olivine and pyroxene, and shrink the fields of spinel and plagioclase, whereas high dry pressure enhances the role of pyroxenes on the liquidus (e.g., Presnall et al., 1979).

The trajectory of $\delta^{18}O$ increase with SiO_2 can be calculated as a small-increment, forward-step model given the identities, proportions, and composition of minerals crystallized, the (changing) composition of melt, and temperature. Whereas there are numerous experiments on mineral-mineral fractionations (see Chacko et al., 2001; Eiler, 2001, for references), there are only a few more difficult CO_2-equilibration experiments on isotope fractionations involving melts of various composition (Stolper and Epstein, 1991; Palin et al., 1996; Matthews et al., 1998; Appora et al., 2003). Nevertheless, these experiments demonstrate that melts can be treated as mixtures of normative mineral components, and thus mineral-melt equilibria can be calculated for a variety of melt compositions. Conveniently, MELTS modeling provides realistic proportions and compositions of minerals and melts, CIPW norms, and enables calculation of isotopic effects at each temperature and fractionation step.

Thus, the particular trajectory of $\delta^{18}O$ change can be modeled as:

$$\delta^{18}O\ (\text{melt})_{j+1} = \delta^{18}O\ (\text{melt})_j + \sum\left((X_i * \Delta_i(T)\right) \qquad (1)$$

where X_i are proportions of differentiating minerals at each step j, and $\Delta_i(T)$ are temperature-dependent and melt composition-dependent, mineral-melt fractionation factors. In addition, the influence of plagioclase composition on melt was recorded, as the change from anorthite to albite produces the strongest (~1‰) effect on $\Delta_{Plag\text{-}melt}(T)$ (e.g., Matthews et al., 1983; Palin et al., 1996); effects of Mg-Fe substitution in mafic minerals on $\Delta_i(T)$ were ignored as being very small (e.g., Hoefs, 1997).

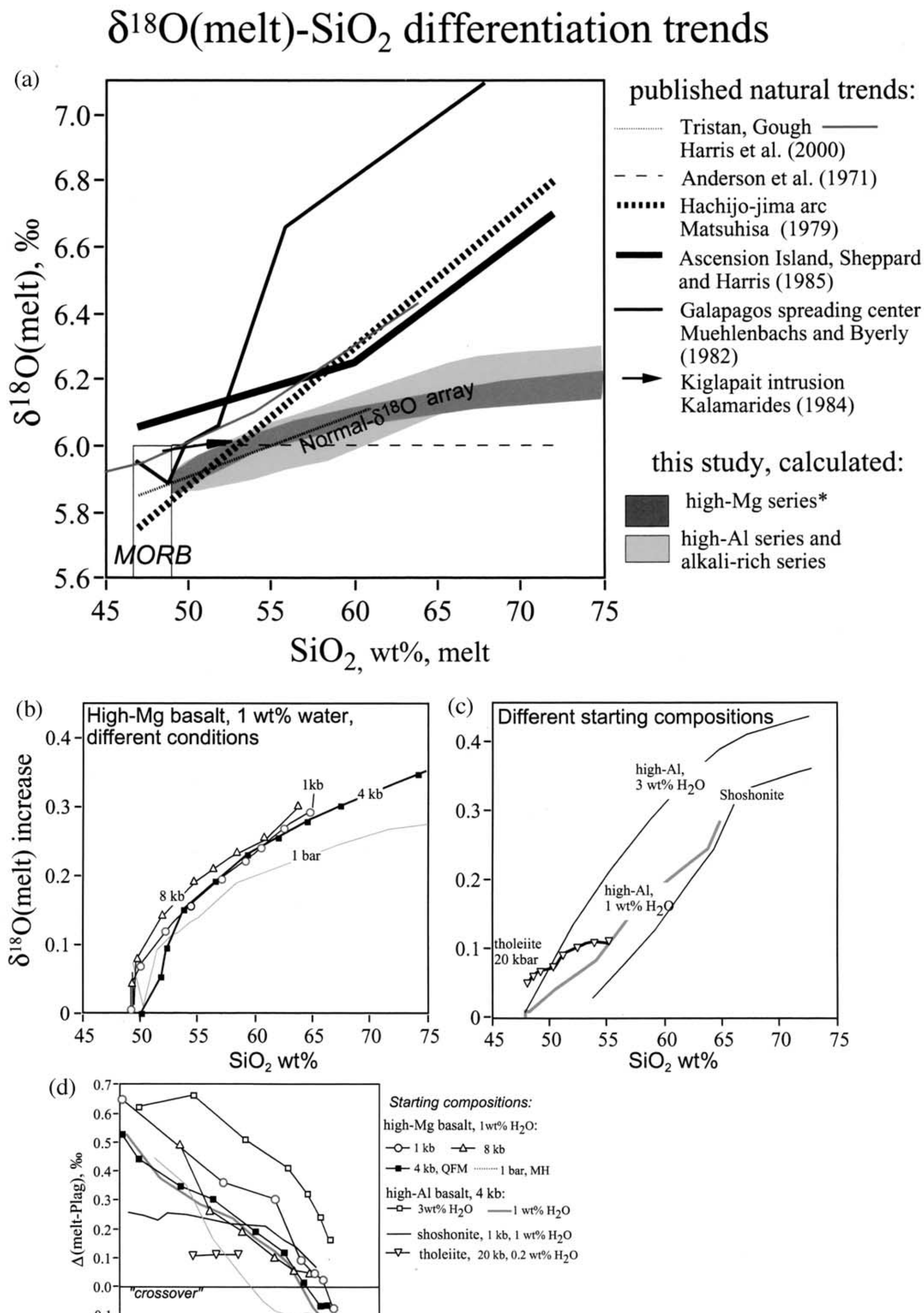

Fig. 4. A-D. Isotopic effects associated with fractional crystallization of basaltic magmas: results of numerical crystallization modeling (MELTS) using starting typical basaltic compositions (high-Mg, high-Al basalts given in Table A2, Electronic Annex, from Volynets, 1994) and isotopic fractionations discussed in text. (A) Trends for high-Al and high-Mg basalts (this study) compared with the compilation of published $\delta^{18}O$ vs. SiO_2 trends. (B, C) Isotopic effects as a function of different conditions of crystallization and starting compositions. (D) Δ(melt-Plag) fractionation as a function of anorthite content of plagioclase; note that a crossover occurs fairly early in differentiation history at 55–60% SiO_2 content of the melt. Kinks are due both to phase appearance and calculation step spacing (typically 10°C).

The results of modeling are presented on Figure 4, and described in more detail in the Appendix. Conclusions can be summarized as follows.

(1) There are a variety of $\delta^{18}O(melt)_{j+1}$ trajectories with increasing degree of differentiation (f%), but they average-out and yield smoothly decelerating (concave downwards curves) increases of $\delta^{18}O$ with increasing SiO_2 of the residual melt (Fig. 4a). Calculated trends, here called normal-$\delta^{18}O$ magma arrays, plot in the middle, but towards the lower end of cited natural estimates, and agree well with recent results for ocean islands (Harris et al., 2000; Eiler, 2001).

(2) Fractional crystallization or melting at high mantle pressures ($p > 15$ kbar) and temperatures yields pyroxene-dominated assemblages and produces negligible effects on residual $\delta^{18}O$(melt) (Fig. 4B). Differentiation at midcrustal pressures (1–8 kb) with olivine and anorthitic plagioclase on the liquidus (typical for island arcs, e.g., Bindeman and Bailey, 1999) yields a maximum 0.3‰ increase. Differentiation of the initially less magnesian magmas, such as shoshonites and high-Al basaltic andesites, yields nearly linear $\delta^{18}O$ vs. SiO_2 trends, and up to 0.45‰ increase from basalt to rhyolite (Fig. 4C).

(3) $\Delta^{18}O$(Plag-melt) changes from a small (−0.1‰) negative value to a progressively more positive (0.3–0.65‰) value as the melt becomes increasingly richer in normative quartz and albite (Fig. 4D). The crossover, inferred from rocks (e.g., Taylor, 1968), occurs at variable compositions of plagioclase —An_{85} to An_{55} for various studied compositions and parameters—and at SiO_2 contents of 55 to 60 wt%. After the crossover, the bulk cumulate assemblage becomes lower in $\delta^{18}O$ than the melt, and this feature persists even after the appearance of quartz. This explains the slightly faster $\delta^{18}O$ vs. SiO_2 increase for initially more differentiated starting compositions. Magnetite, as a minor phase, produces only a small (ca. <0.05‰) effect on $\delta^{18}O$(melt), even in oxidizing conditions.

(4) The results of this modeling are in good agreement with the magnitudes and values of $\delta^{18}O$(melt) vs. SiO_2 and plagioclase crossover relationships of concurrently published increment method calculation by Zhao and Zheng (2003).

Given the above definition of a "normal-$\delta^{18}O$ differentiation array" (changing from 5.8 ± 0.2‰ for parental basalts to 6.1 ± 0.3‰ for rhyolites at ~90% differentiation, Fig. 4A), any magma with lower values is here called low-$\delta^{18}O$, and any magma above the differentiation array is called high-$\delta^{18}O$. High-$\delta^{18}O$ values cannot be produced by closed-system evolution from a mantle-derived arc basalt, and are generally derived from high-$\delta^{18}O$ source rocks (e.g., supracrustals), or result from addition of a high-$\delta^{18}O$ component (e.g., slab or crustal fluids) to magma generation sources. Low-$\delta^{18}O$ magmas reflect assimilation or melting of low-$\delta^{18}O$ rocks altered at high-T by surface water.

4.2. Isotopic Fractionations and $\delta^{18}O$ of Melt in Equilibrium with Minerals

Table 1 presents $\delta^{18}O$ values for phenocrysts from 111 eruptive units of 30 volcanic centers of Kamchatka and Kuriles. Sample descriptions and ages of units are given in Table A1 (Electronic Annex). The $\delta^{18}O$ values of coexisting minerals are plotted in Figure 5. On the basis of experiments (Chiba et al., 1989), small $\Delta^{18}O$ indicate equilibrium at magmatic temperatures suggesting that $\delta^{18}O$ values of phenocrysts reflect quenched magmatic conditions. There is a spread of >3‰ in magmatic $\delta^{18}O$ values for each mineral. Twenty eight plagioclase-clinopyroxene pairs yielded a fractionation of 1.18 ± 0.37‰ (1st dev). Nineteen plagioclase-amphibole fractionations produced comparable fractionation 1.23 ± 0.30‰ (1 st dev). The $\Delta^{18}O$(Cpx-Amph) can therefore be estimated to be 0.05‰, and this agrees well with estimates by Kohn and Valley (1998) of 0.1 ± 0.2‰ at 800°C. Such $\Delta^{18}O$(Cpx-Amph) fractionation was assumed in calculations of $\delta^{18}O$(melt) below. Nine plagioclase-olivine pairs yielded 0.72 ± 0.33‰, in good agreement with data of Eiler et al. (2000b) on lavas from other island arcs. Xenocrystic and protocrystic olivines that result from preeruptive disintegration of olivine-anorthite cumulate nodules, and magma mixing (e.g., Izbekov et al., 2002), occur sporadically; and are excluded from the calculation of $\delta^{18}O$(melt). Each Δ(min-melt) value is a function of melt composition, mineral composition, and temperature. We used $\delta^{18}O$ for pyroxene, amphibole, olivine, quartz, and plagioclase to independently calculate $\delta^{18}O$(melt), after the following procedure.

Derivation of the $\delta^{18}O$ value of melt (and magma) in equilibrium with phenocrysts is a necessary and precise procedure, since whole-rock analyses of volcanic rocks often prove to be unreliable for inferring primary magmatic values. Coexisting mineral pairs allow estimation of $\delta^{18}O$ values of magma at temperatures and melt compositions using the above experimental fractionation factors. Increasing SiO_2 content of the melt is accompanied by a temperature decrease from ~1200°C to ~800°C. The decrease in anorthite content of plagioclase is from ca. An_{80} (basalts) to An_{30} (rhyolites), and there is a simultaneous, but less significant decrease in Mg/Fe ratio of pyroxenes and amphiboles from 0.8 to 0.6–0.5. Crystallization modeling yielded SiO_2, T, and An content of plagioclase (e.g., Fig. 4), and CIPW norms of melt. A robust linear parameterization of T, SiO_2, and An content of plagioclase was assumed to match the observed variations and results (Table A2 and Fig. A1 in Electronic Annex). Next, a relevant subpermil fractionation factor was added (or subtracted) to measured $\delta^{18}O$ values of Fe-Mg minerals, plagioclase, and quartz to calculate $\delta^{18}O$ value of melts, in accordance with SiO_2 contents of each composition that indirectly include temperature dependence.

An internal check of MELTS calculations is achieved by comparing calculated $\delta^{18}O$(melt) with measured $\delta^{18}O$(WR) in fresh rocks (Table 1). The difference: $\delta^{18}O(calc.) - \delta^{18}O(meas.) = 0.02 \pm 0.34$‰ ($n = 6$) suggesting no introduced bias in inferring $\delta^{18}O$(melt) from phenocrysts. The resulting $\delta^{18}O$(melt), based on different minerals, plot within a range of ± 0.2‰ and were averaged to obtain the preferred $\delta^{18}O$(melt). Note that $\delta^{18}O$(melt) is different from $\delta^{18}O$(magma) since the latter is dependent on the % of crystals and melt (i.e., magma = melt+phenocrysts). However, the proportion of crystals in Kamchatkan volcanic rocks is relatively small (<20 vol%), and Δ(mineral-melt) fractionations often show small, opposite signs. It is therefore safe to assume that for near-liquidus rocks $\delta^{18}O$(melt) is equal to $\delta^{18}O$(magma), though possibly 0.1‰ higher than magma represented by crystal-rich samples.

Table 1. Oxygen isotope composition of phenocrysts in Kamchatkan volcanic rocks. See Table A1 (internet repository) for description of eruptive units and whole-rock analyses. SiO_2 and K_2O given here are LOI-free.

	SiO_2	K_2O	$\delta^{18}O$, permil									$^{87}Sr/^{86}Sr$
Sample	wt%	wt%	Qz	Pl	Amph	Cpx	Opx	Mt	Ol	Glass	magma (calc)	
Shiveluch												
97044/1	62.44	1.53		7.30	5.68						7.14	
97051/2	59.11	1.32		7.30	5.58						6.99	
SH-3	57.04	0.99		7.08	5.53						6.80	
96025/4	60.03	1.37			5.50						6.75	
97049/2	57.11	1.10			5.83						6.99	
1189/1	50.16	1.68								6.95	6.95	0.703673
OOK37	53.83	0.91		6.83							6.56	
97058/2	53.40	0.96		7.26		5.71					6.75	
5734	51.01	1.67			6.36				5.83		6.76	0.703703
5764	53.87	1.28							5.61, 5.68		6.08	0.70347
B544/N	47.23	0.72								7.49, 6.92		0.70341
B541/2v	54.71	1.19		6.56	5.87	5.27					6.05	0.70335
B547	60.95	1.30		7.15	5.72						6.64	0.70335
B548b	62.58	1.47		7.79	6.05	5.31					7.49	0.70341
Bezymianny												
B580	58.91	1.49		7.97		7.01				7.72, 8.29	7.88	0.70361
B574/A	56.00	1.09								7.27		0.70358
B-584	64.62	1.42								7.51		0.70359
B600	55.81	1.11		7.56	6.81	6.61						0.70354
Tolbachik												
TOL-2	50.85	0.88				5.63			5.52	5.69	6.22	0.70344
Teklentunup												
7305	57.97	4.56		4.85		3.74					4.70	0.70366
1019/1	50.16	1.85							5.52		5.83	0.70366
Kizimen												
80013/4	63.62	1.89		7.21	5.63						7.11	0.703307
K35/1	63.72	1.49		7.02	6.19						7.30	
Khangar												
98032/4	69.26	2.56		6.95	5.54						7.14	0.70343
98032/2	68.41	2.36		6.61	5.75						7.01	0.70338
Uzon												
87L-103	66.10	1.57		4.73		3.66, 3.74					4.84	0.703297
99L-101	68.06	2.00		4.67		3.10					4.59	0.703346
D493-74	72.24	3.52		4.98		4.57, 4.29					5.61	0.703494
D388i-74	71.62	2.17		4.88							5.14	0.703369
D368-74	71.74	1.98		4.44	3.13						4.72	0.703357
W-11	65.99	1.30		4.75		3.36					4.70	0.7035
Maly Semyachik												
5230/1	66.78	2.00		4.49		3.20				4.51	4.55	0.703193
Bol Semyachik												
90L-8	64.07	1.99		6.34		5.21					6.36	0.703443
84L-103	70.53	1.94	7.47	6.57							6.70	0.703444
Karymsky												
808 KAR 4	67.26	2.45		5.02		3.88					5.13	0.703198
KRM 5ab-4	72.59	2.93		4.86							5.15	0.703181
99IPE-4	69.58	2.37		5.25		3.56					5.16	
99IPE-8	62.30	1.56		5.36		4.32					5.37	
99IPE-22a	52.38	0.59		4.84		4.27			4.48	5.36	4.85	
99IPE-12	60.41	1.30		5.44		4.38					5.39	
99IPE-6	69.54	2.45		4.92		4.01					5.22	
J4257	75.93	3.37								3.42	3.42	
Avachinsky												
99201/1	60.66	0.92		7.06	5.95						7.22	0.703374
99163/9	53.02	0.70		7.10	6.00						7.04	0.703459
29135	57.22	0.70			5.61						6.78	
29215	50.95	0.70				5.89			6.10		6.54	
TOL-3	51.85	0.37								6.49		0.70335
Koryaksky												
26061	50.12	0.91							5.85		6.16	
26018	58.96	1.63				6.12						
26129	55.20	1.50				5.82						

(Continued)

Table 1. (Continued)

	SiO_2	K_2O	$\delta^{18}O$, permil								$^{87}Sr/^{86}Sr$	
Sample	wt%	wt%	Qz	Pl	Amph	Cpx	Opx	Mt	Ol	Glass	magma (calc)	
Chasha Crater												
98KAM2.3	72.63	3.46		7.50, 7.70							7.89	
Opala												
Barany amphiteatre Crater												
98 KAM 2.4	73.68	3.65		7.06							7.38	0.7033
Summit Crater												
98-33/2	65.54	2.87		6.84	5.96						7.15	0.703179
98-10	73.64	3.55		7.34, 7.44, 7.46							7.70	
Gorely												
3667	64.77	2.64				4.44				5.22	5.44	0.70324
Mutnovsky												
B618/3	50.02	0.37								5.93		0.70338
B615/B	51.52	0.53								5.82		0.70315
B610A	59.49	1.69								5.7, 5.57		0.70338
B615A	51.52	0.53								6.43, 6.07		0.70329
Nachiki												
TOL-4	75.59	4.49		7.91						8.55	8.51	0.70365
Ksudach												
8882/2	68.45	1.48		5.56		4.66, 4.56					5.80	0.703276
C999	54.18	0.62		5.15		4.21					4.97	0.703311
8880/5	71.78	1.57		4.68, 4.69		3.46					4.89	0.703389
C953	65.35	1.20		4.75			3.74		4.53		4.87	0.70337
86039/14	62.57	1.15		5.02		3.71					5.01	
C918a	62.44	1.06		5.64					4.64		5.62	0.703312
8889/2	69.55	1.51		4.92		3.96					5.19	
8889/3	62.79	1.14		5.12							5.11	
Ks-alliw	50.00			5.20					4.63		5.33	0.70331
C977a	63.22	1.15		5.01			4.09				5.11	
C977	64.75	1.16		4.94							4.99	0.703318
KA-38a/7	49.35	0.22								5.84		0.70331
KA110-7	58.68	0.77								5.41		0.70322
KA25A-7	67.15	1.20								5.09		0.70325
KA39/7	48.21	0.19		5.62		4.43					5.06	0.70339
KA1/7	56.79	0.64								5.74		0.70326
Pauzhetka												
83L20	71.14	2.96	7.15	6.04							6.52	0.703255
Kurile Lake												
KAM-03a	73.82	1.90		5.73, 5.51	4.38			2.05, 2.06			5.90	0.703312
KAM-29AB	54.63	0.49		5.23	4.16			3.07			5.11	0.703251
KL-1	68.90	1.66		5.35	4.21						5.73	0.703347
KL-2	56.52	1.34		5.59		4.60					5.40	0.703281
97KAM-02	69.52	1.76			4.37	4.35					0.00	
97KAM-11	72.81	1.86		5.41		4.21					0.00	
97KAM-29B1	66.64	1.48		5.55	4.24	4.32					0.00	
97KAM-29AL	71.38	1.91		5.43	4.12						0.00	
86680	64.65	1.31		5.68		4.67					5.78	
Iiyinsky Volcano												
650	64.40	1.56		4.52		3.83					4.77	
621	59.88	1.26		4.96		3.85					4.87	
615	52.37	0.57								5.30	4.98	
96K8-14	51.92	0.46		4.92		3.36					4.36	
96K8-24	59.47	1.13		4.95							4.84	
8645/1	63.41	1.47		5.00							5.01	
Zheltovsky Volcano												
CI-114	50.00			5.72					5.24		5.43	
Dikii Greben Volcano												
B319-1	65.11	1.49	7.42	5.85							6.15	0.70323
B318-1	67.45	1.69	7.29	5.85							6.15	0.70322
B333-1	52.71	0.87		6.09							5.78	0.70322
B319-6	64.79	1.38		5.63							5.68	0.70322
B325-1	54.77	0.82	7.31								5.96	0.70318
B325	65.30	1.45	7.35								6.32	0.70322
B334	70.63	2.20	7.27								6.40	0.70322

(Continued)

Table 1. (Continued)

	SiO_2	K_2O	$\delta^{18}O$, permil								$^{87}Sr/^{86}Sr$	
Sample	wt%	wt%	Qz	Pl	Amph	Cpx	Opx	Mt	Ol	Glass	magma (calc)	
Kurile Island Arc												
Golovnin Caldera (Kunashir)												
416-4	64.57	0.42	6.82			4.54					5.70	
G-117	64.57	0.42				4.93					6.09	
116b	49.97	0.13							4.85		5.16	
116-1a	49.97	0.13				5.10			5.02		5.57	
Zavaritsky Volcano (Simushir)												
ZAV-1	67.01	0.65		5.86					4.88		5.84	
Mendeleev Volcano (Kunashir)												
7587	56.32	0.20	6.76								5.75	
7585	75.95	0.99	6.99	6.07							6.46	
Kudriavy Volcano (Iturup)												
B605	57.93	0.57							5.39		5.94	
Bogdan Khmeinitsky (Iturup)												
B535	56.03	1.42		6.03					5.08		5.70	
Alaid Volcano (Atlasov)												
92-223	48.50	1.72		6.34					5.17		5.66	
Brouton Volcano (Brouton)												
B15-307	58.22	2.10		6.06		5.02			5.29		5.92	0.70306

**Calculated using $\delta^{18}O$ values of phenocrysts and inferred mineral-magma fractionation (see text).

5. RESULTS

5.1. $\delta^{18}O$ Values of Volcanic Rocks

Table 1 presents best estimates of $\delta^{18}O$(magma) in Kamchatkan volcanic rocks and these are used in combination with other isotopic systems below.

5.1.1. High-$\delta^{18}O$ Basic Rocks of Kamchatka

Basic rocks of Kamchatka are either normal-$\delta^{18}O$, or high-$\delta^{18}O$ (Fig. 6, Table 1) whereas low-$\delta^{18}O$ basalts are absent (Fig. 3). Dorendorf et al. (2000) reported high-$\delta^{18}O$ values for olivines and pyroxenes of Klyuchevskoy volcano, the largest

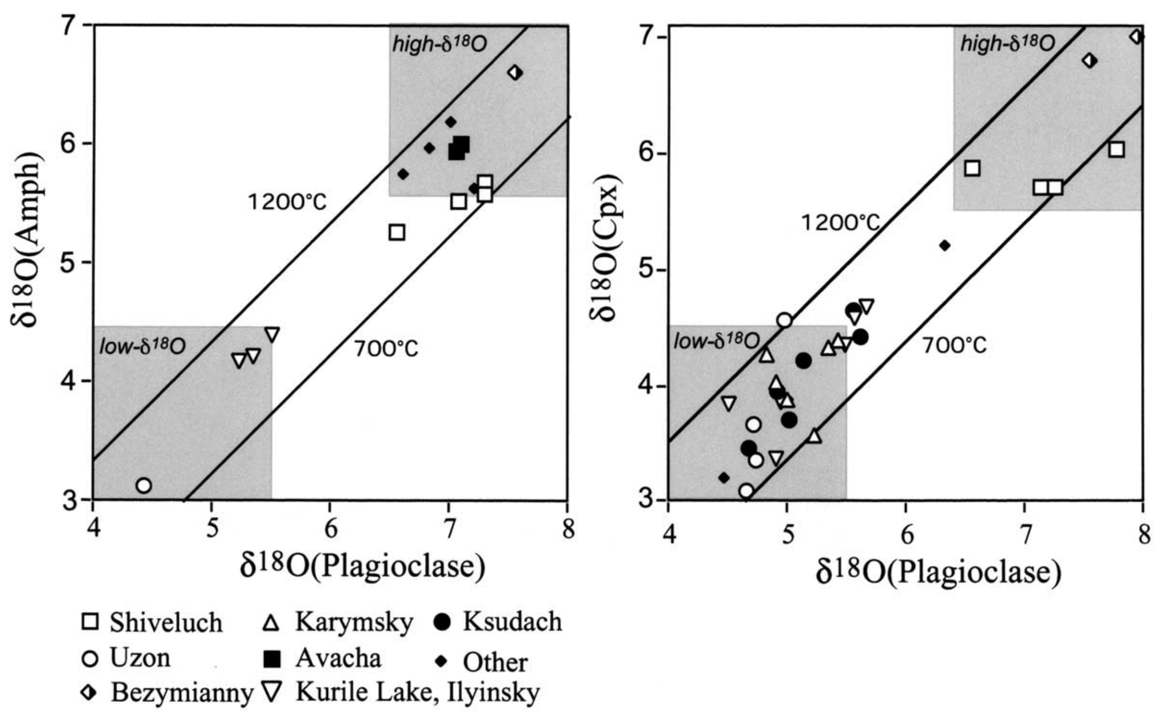

Fig. 5. $\delta^{18}O$(Plag) vs. $\delta^{18}O$(Cpx, Amph) showing the range of $\delta^{18}O$ values in Kamchatkan magmas. Note that isotopic fractionations are consistent with equilibration at magmatic temperatures. Experimental Δ(Plag-Cpx) fractionations are from Chiba et al. (1989) for An_{50} at 1200°C, and An_{30} at 700°C, Δ(Plag-Hb) are 0.1‰ larger. Specified volcanoes are discussed in the text. Fields for high- and low-$\delta^{18}O$ magmas are shown for comparison. Notice that low-$\delta^{18}O$ samples are predominantly clinopyroxene-bearing, while high-$\delta^{18}O$ samples are amphibole-bearing.

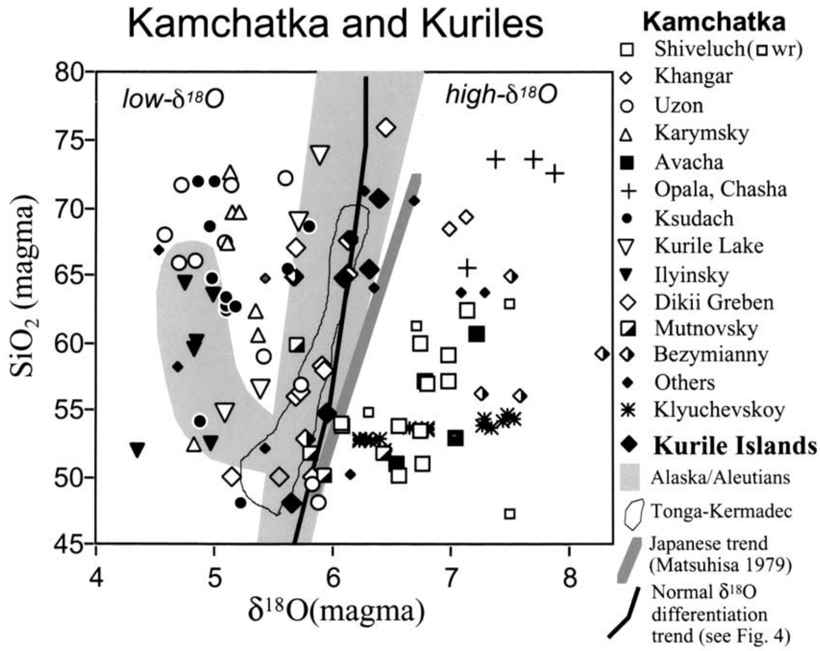

Fig. 6. $\delta^{18}O$(magma) vs. SiO_2 content for volcanoes of Kamchatka; the $\delta^{18}O$(magma) is calculated from the $\delta^{18}O$ values of phenocrysts, see text. The thick line is a calculated normal-$\delta^{18}O$ array, see Figure 4A. The shaded field shows normal-$\delta^{18}O$ (mantle magma fractionation trend), and low-$\delta^{18}O$ magmas (area with negative slope, Unimak and Umnak islands) for the Aleutian and Alaskan magmas (Bindeman et al., 2001); hatched line is a trend for Japanese volcanoes (Matsuhisa, 1979). Tonga-Kermadec data are within thin line area (I. N. Bindeman et al., unpublished data). Note that more than half of Kamchatkan volcanoes plot in the field of low-$\delta^{18}O$ magmas, and other half in the field of high-$\delta^{18}O$ magmas. Lower latitude circum-Pacific arcs are normal-$\delta^{18}O$.

volcano of Eurasia. The present work greatly expands the number of mantle-derived basalts of Kamchatka with a high-$\delta^{18}O$ signature. High-$\delta^{18}O$ basalts and basaltic andesites are characteristic of Bezymianny, Shiveluch, Avachinsky, and Koryaksky volcanoes. Additionally, we have analyzed a suite of 25 magnesian olivines (Fo_{90}) from the most primitive basalts from 14 volcanoes and monogenetic cones throughout Kamchatka supplied to us by Dr. M. Portnyagin. The olivine $\delta^{18}O$ values range from 5.3 to 6.8‰, and individual results will be reported elsewhere. High-$\delta^{18}O$ magmatic values in intermediate and silicic rocks characterize differentiated products of Khangar, Opala, Chasha, and Kizimen volcanoes. Therefore, high-$\delta^{18}O$ values are not constrained to the Central Kamchatka Depression but also characterize volcanoes in the Eastern Volcanic Front (e.g., Avachinsky, Koryaksky, and Opala), and on the Sredinny Range (Khangar).

5.1.2. *Low-$\delta^{18}O$ Silicic Magmas of Kamchatka*

In contrast to basalts, the studied intermediate to silicic rocks, as well as mafic cumulates and mafic rocks associated with some calderas, from 100 units of 23 volcanic centers have unusually low-$\delta^{18}O$ and plot below the normal-$\delta^{18}O$ fractionation trend (Fig. 6). Such a great abundance (by number of units and by volume) of low-$\delta^{18}O$ magmas makes Kamchatka one of the largest Quaternary low-$\delta^{18}O$ volcanic areas on Earth. Only Iceland has similar, large areas of low-$\delta^{18}O$ volcanics (Muehlenbachs et al., 1974; Condomines et al., 1983; Taylor and Sheppard, 1986; Hemond et al., 1988). The lowest $\delta^{18}O$ values in Kamchatka (~4.5‰) are found in voluminous Uzon rhyodacitic ignimbrites and intracaldera volcanics (see Table 2). This value is 1.5–2‰ lower than the estimated value of ca.

Table 2. Robust linear approximations of Δ(min.-melt), SiO_2(wr), T°C, and An% relations based on 75 compositions in six crystallization experiments (see Appendix for plotted data).

Δ (min.-melt) = a[SiO2 wt%] + b	a	b
Clinopyroxene	0.061	−2.72
Olivine	0.088	−3.57
Plagioclase	0.027	−1.45

Δ (min.-melt) = c[T°C] + d	c	d
Clinopyroxene	−0.0033	4.16
Olivine	−0.0048	6.42
Plagioclase	−0.0016	1.75

Δ (min.-melt) = e[An%] + f	e	f
Clinopyroxene	−0.024	2.37
Olivine	−0.034	3.75
Plagioclase	−0.010	0.78

T(°C) = −17.2[SiO2 wt%] + 2014; An% = 0.128[T°C] −64.99; An% = −2.435[SiO2 wt%] + 206.25.

6.1 ± 0.3‰ for normal-$\delta^{18}O$ rhyodacites and rhyolites, but 3‰ lower than basic magmas from typical high-$\delta^{18}O$ Kamchatkan sources.

We find that there is no regional or geodynamic control on the appearance of low-$\delta^{18}O$ silicic magmas. Neighboring volcanoes often do not show any ^{18}O-depletion (see Fig. 1, Table 1). There is no Kamchatka-wide correlation of $\delta^{18}O$ with K_2O or SiO_2 or any other chemical or isotopic parameters (see below). However, the specific values of these parameters, in these low-$\delta^{18}O$ centers, provide a valuable discrimination of different tephra layers and the products of major caldera-forming eruptions. Most low-$\delta^{18}O$ magmas tend to be pyroxene-bearing and amphibole-free (Table 1, Fig. 5), suggesting lower water content in parental magmas, and/or remelting at shallower depths. High-$\delta^{18}O$ magmas are, on the contrary, predominantly amphibole bearing. This important observation goes against the intuitive understanding that low-$\delta^{18}O$ magmas should be richer in water, and thus lower in $\delta^{18}O$. Skaergaard low-$\delta^{18}O$ gabbros are not noticeably richer in hydrous minerals (Taylor and Sheppard, 1986).

5.1.3. Calderas vs. Stratovolcanoes, and Low-$\delta^{18}O$ Magmas

The great majority of voluminous low-$\delta^{18}O$ magmas appear in calderas, and especially multicaldera volcanoes (Table A1, Electronic Annex, and Table 1) varying in age from Early Pleistocene to historic (Sheymovich, 1979; Erlich, 1986; Fedotov and Masurenkov, 1991), though not all calderas contain low-$\delta^{18}O$ magmas. Thus, it seems that the necessary condition for normal- to high-$\delta^{18}O$ mantle-derived magmas to acquire a low-$\delta^{18}O$ signature in the Kamchatkan crust is a shallow magma chamber. The latter condition is characteristic of calderas; under stratovolcanoes, magma chambers are likely to be deeper, less evolved, and shorter-lived. Since large shallow magma chambers often contain silicic differentiates, the low-$\delta^{18}O$ values characterize primarily silicic magmas. Additionally, a caldera is an important enclosed hydrogeological locus for the development of a geothermal system driven by a high heat flux. It seems that the existence of an older overlapping or enclosing caldera (e.g., Ksudach volcano, Volynets et al., 1999) which hosted an earlier hydrothermal system before the most recent caldera event, is an important factor in the appearance of low-$\delta^{18}O$ magmas.

For two multicaldera volcanic centers—Pauzhetka-Kurile Lake-Ilyinsky, and Ksudach—considerable ^{14}C age data are available (Table A1, Electronic Annex). The $\delta^{18}O$ values for phenocrysts and magmas when plotted against age exhibit variations in $\delta^{18}O$ between different eruptive units of the same volcanic system (Fig. 7), suggesting a shallow origin of the magmas and their low-$\delta^{18}O$ values. Mafic cumulates, and the products of zoned silicic-mafic ignimbrite eruptions, have comparable levels of $\delta^{18}O$ depletion in the first-erupted silicic portions and in subsequent more mafic portions (Table 1), similar to what is observed in the zoned basaltic andesite-dacite Fisher and Okmok eruptions in the Aleutians (Bindeman et al., 2001). This implies that the hot basic magmas that initiated melting or mixing had enough time to exchange oxygen in the upper crustal magma chamber.

5.1.4. Major Holocene Calderas and Volcanoes of the Kurile Island Arc

We analyzed $\delta^{18}O$ in minerals from caldera-forming eruptions of several volcanoes and the largest (>10 km) Holocene calderas (Zavaritsky and Golovnin) of the Kurile island arc (Table 1; Table A1, Electronic Annex). Silicic and basic rocks of historic and radiocarbon-dated eruptions—Mendeleyev, Bogdan Khmelnitsky, Kudriavy, Brouton, and Alaid stratovolcanoes—were also studied. In sharp contrast to Kamchatka, all analyzed samples of the Kurile island arc, from caldera or stratovolcano, represent normal-$\delta^{18}O$ magmas. Radiogenic isotope systematics of the Kurile island arc (Bailey et al., 1987; Zhuravlev et al., 1987; Bindeman and Bailey, 1999) are consistent with derivation of a compositionally-diverse basaltic suites (tholeiitic, calc-alkaline, and shoshonitic) from a mantle source that is 1) changing from ultra-depleted to depleted; 2) has negligible contribution from sediments (Tera et al., 1990; Ryan et al., 1995), and 3) has small contribution from slab fluids.

5.2. $\delta^{18}O$ vs. Other Isotope Systems

Table 3 contains analyses of Sr, Nd, and Pb isotopes performed by us on the suite of studied samples; additional $^{87}Sr/^{86}Sr$ ratios for the same units or the same samples are taken from the published sources (see Fig. 3B). The $\delta^{18}O$(magma)-radiogenic isotope correlations are plotted on Figures 8 and 9, and lead to following observations.

1) Regardless of SiO_2 content, Pb and Nd isotopic ratios in all studied Kamchatka volcanics, including the most differentiated products of caldera-forming eruptions (Tables 1 and 3), plot within the range of normal Pacific MORB, as do Kurile island arc volcanics (Bindeman and Bailey, 1999). $^{143}Nd/^{144}/Nd$ shows no trends with $\delta^{18}O$ (Fig. 9C) and there is a scattered relation between $^{143}Nd/^{144}/Nd$, $^{206}Pb/^{204}Pb$, $^{208}Pb/^{204}Pb$, $^{207}Pb/^{204}Pb$ and SiO_2 (not plotted). In EVF, at Ksudach and Kurile Lake, the more differentiated products are only slightly more radiogenic than mafic rocks (Bindeman and Bailey, 1994). A variability of 0.0002–0.0003 Sr units exists for the Khangar volcanic center (Dril et al., 1999), and is explained by assimilation of radiogenic metamorphic basement.

2) $^{87}Sr/^{86}Sr$ ratios in mafic Kamchatkan volcanics are higher than those in Pacific MORB, and show an overall positive correlation with $\delta^{18}O$ (Fig. 8B). The trend is particularly apparent for normal- to high-$\delta^{18}O$ rocks of CKD: Klyuchevskoy, Bezymianny, Zarechny, Kharchinsky, and Shiveluch volcanoes. Remarkably, there is a negative correlation of $^{87}Sr/^{86}Sr$ with $\delta^{18}O$ for low- to normal-$\delta^{18}O$ rocks, that tend to be silicic in composition (Figs. 8A,C). This trend is apparent for Kurile Lake, Ksudach, and Uzon, all in the EVF with a regionally similar $^{87}Sr/^{86}Sr$ ratio in parental basalts. A similarly negative trend is observed in rift-derived tholeiites from Iceland; this suggests that the ambient Icelandic crusts and Kamchatka's are older, more radiogenic, and are more depleted with respect to $\delta^{18}O$ (down to -10‰, Hattori and Muehlenbachs, 1982; Hemond et al., 1988, although bulk is probably 0 ± 3‰). Lead isotopic signatures for the same Kamchatkan eruptive units

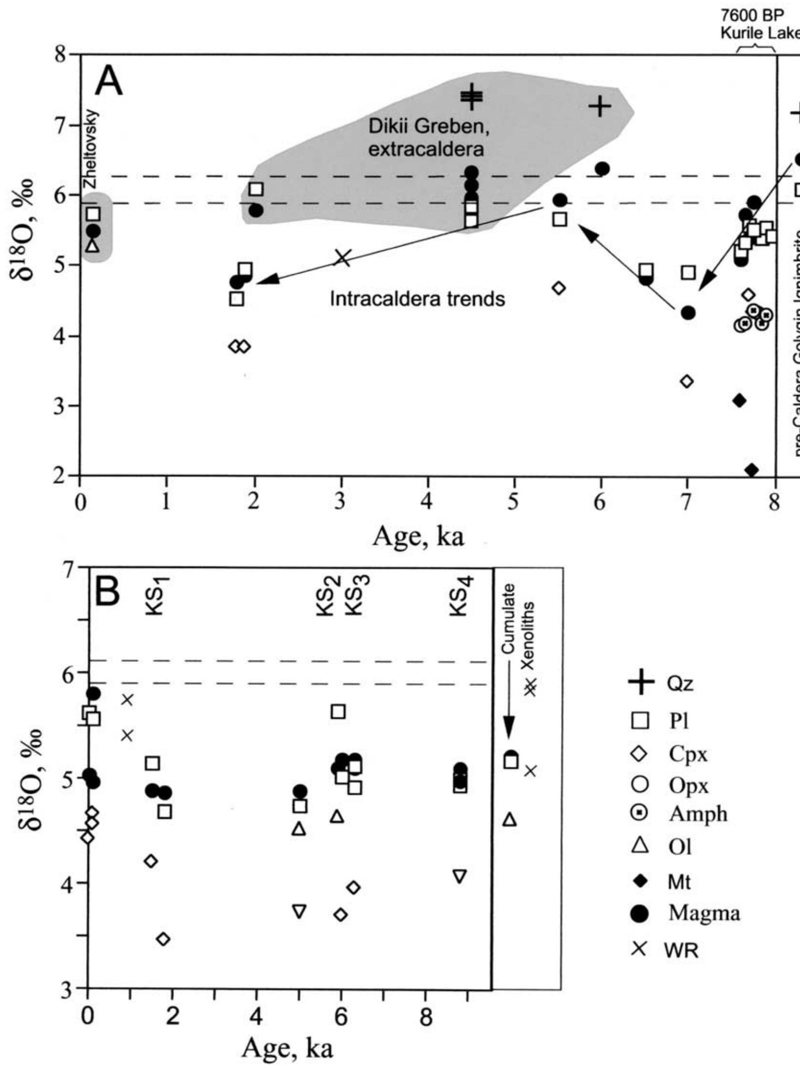

Fig. 7. Evolution patterns for two caldera complexes: Kurile Lake (A) and Ksudach (B). Data are from Table 1; see Table A1 (Electronic Annex) for description and ^{14}C ages of eruptive units. Dashed lines delineate the field of normal-$\delta^{18}O$ silicic magmas. Olivines (Fo_{75}) in Ksudach are xenocrysts derived from preeruptive disintegration of olivine-anorthite cumulates. See Erlich (1986), Macias and Sheridan (1995), Volynets et al. (1999), Rinkleff (1999), and Ponomareva et al. (2004) for geology and geochemistry of these caldera complexes.

(Figs. 9A,B) show a more subdued negative correlation, and suggest that most assimilants are also slightly more radiogenic with respect to lead isotopes.

(3) Dredged sediments in front of the Kamchatka arc (silicic ooze, altered basalts, and mud) have expectedly high $\delta^{18}O$ (9 to 23‰), and $^{87}Sr/^{86}Sr$ values (Table 4), and also show positive correlation. On bulk average, however, both O and Sr isotope values are only moderately high in sediments. Other isotope analyses of sediments in NW Pacific (see Bailey, 1993, 1996; Kersting and Arculus, 1995; Plank and Langmuir, 1998) are similar to our near-Kamchatka values.

(4) Radiogenic isotopes when plotted against each other highlight regional differences between volcanics in the CKD and EVF. CKD volcanics are least radiogenic with respect to Pb and Nd isotopes, but span an equal or even somewhat larger range in Sr and O isotopes. On $^{87}Sr/^{86}Sr$ vs. $^{143}Nd/^{144}/Nd$ (Fig. 9D) Kamchatka volcanics point toward Pacific sediments; $^{206}Pb/^{204}Pb$ vs. $^{208}Pb/^{204}Pb$ and $^{207}Pb/^{204}Pb$ (Figs. 9E,F) plot slightly above the Pacific MORB field, towards the Indian MORB. MORB-like Pb isotopic signatures (e.g., Kersting and Arculus, 1995), and other geochemical monitors of Kamchatkan volcanics, are consistent with negligible sediment-control (<1–2% sediments) on Sr and O isotopic systematics in volcanics. At face value, the more primitive compositions of Pb and Nd in CKD suggest smaller involvement of slab sediments in the petrogenesis of CKD magmas (e.g., Churikova et al., 2001); elevated values of $^{87}Sr/^{86}Sr$ in voluminous volcanism in CKD can be interpreted to represent fluid addition with small concentration of Pb and Nd (e.g., Dorendorf et al., 2000). We note here that the isotopic analyses of this study, as well as those reported for predominantly mafic volcanics by Churikova et al. (2001) and Kepezhinskas et al. (1997), overlap and

Table 3. Whole-rock radiogenic isotope analyses of selected Kamchatkan volcanic units. See Tables 1, and A1 for description.

Volcano	SiO_2 (WR)	$^{87}Sr/^{86}Sr$	$^{206}Pb/^{204}Pb$	$^{207}Pb/^{204}Pb$	$^{208}Pb/^{204}Pb$	$^{143}Nd/^{144}Nd$
Shiveluch						
B544/N	47.23	0.70341	18.258	15.491	37.901	
B541/2v	54.71	0.70335	18.331	15.509	37.945	0.513140
B547	60.95	0.70335	18.362	15.493	37.932	
B548b	62.58	0.70341	18.304	15.490	37.885	0.513097
Bezymianny						
B580	58.91	0.70361	18.057	15.502	37.753	
B574/A	56.00	0.70358	18.251	15.488	37.862	0.513090
B-584	64.62	0.70359	18.267	15.491	37.891	0.513100
B600	55.81	0.70354	18.261	15.496	37.935	
Tolbachik						
TOL-2	50.84	0.70344	18.356	15.564	38.035	0.513075
Uzon						
87L-103	61.10	0.703297	18.376	15.515	38.095	0.513071
99L-101	67.53	0.703346	18.376	15.515	38.099	0.513066
D493-74	72.10	0.703494	18.332	15.501	38.033	0.513067
D388i-74	71.40	0.703369	18.367	15.520	38.110	0.513070
D368-74	70.96	0.703357	18.361	15.507	38.075	0.513072
W-11	65.99	0.703500				
Maly Semyachik						
5230/1	66.78	0.703193	18.389	15.498	38.051	0.513111
Bolshoi Semiachik						
90L-8	63.82	0.703443	18.365	15.513	38.091	0.513035
84L-103	70.64	0.703444	18.379	15.501	38.067	0.513065
Avachinsky						
TOL-3	51.85	0.703350	18.427	15.526	38.155	0.513070
Mutnovsky						
B618/3	50.02	0.70338	18.358	15.520	38.141	0.513113
B615/B	51.52	0.70315	18.333	15.498	38.073	
B610A	59.49	0.70338	18.350	15.500	38.110	0.513060
B615A	51.52	0.70329	18.340	15.507	38.099	
Nachiki						
TOL-4	75.59	0.70365				0.513028
Ksudach						
C977	62.99	0.703318	18.319	15.496	38.093	
KA-38a/7	49.35	0.70331	18.350	15.521	38.163	0.513070
KA110-7	58.56	0.70322	18.043	15.585	38.098	
KA25A-7	67.15	0.70325	18.349	15.500	38.117	0.513063
KA39/7	48.21	0.70339	18.568	15.528	38.091	
KA1/7	56.79	0.70326	18.095	15.572	37.945	
Pauzhetka						
83L20	70.34	0.703255	18.358	15.504	38.141	0.513056
Kurile Lake						
KL-1	68.94	0.703347				
KL-2	56.52	0.703281				

2σ uncertainties: $^{87}Sr/^{86}Sr$: $\pm$ 0.00001; $^{206}Pb/^{204}Pb$ and $^{207}Pb/^{204}Pb$: $\pm$ 0.01; $^{208}Pb/^{204}Pb$; $\pm$0.02; $^{144}Nd/^{143}Nd$: $\pm$0.000005.

demonstrate that regardless of SiO_2 content they also lie in the field of lower and upper crustal sources of Mesozoic to Miocene age.

5.3. Correlation with Crustal Thickness and Slab Depth

Isotopic compositions of oxygen and strontium when plotted against the slab depth (Figs. 10C,D) demonstrate an overall positive correlation for Kamchatka (with the exception for Shiveluch which is built on a thinned crust). This departs from the negative correlation of $^{87}Sr/^{86}Sr$ vs. depth, and no dependence for $\delta^{18}O$ vs. depth, in the Kurile island arc, a southern extension of the same subduction zone that is built upon far thinner crust (20–30 km); the petrogenesis there is interpreted to be dominated by mantle processes (e.g., Bindeman and Bailey, 1999, and references therein). When plotted against crustal thickness (Fig. 10 A,B) $^{87}Sr/^{86}Sr$ and $\delta^{18}O$ exhibit significant scatter; mafic volcanics in the EVF show a scattered positive correlation with crustal thickness, whereas silicic volcanics from the same volcanoes and crustal thickness lose this trend. Similar poor trends are observed in isotopic variations of Nd and Pb (not plotted; see Table 3 and Fig. 9).

Radiogenic isotope ratios for mafic volcanics (Figs. 8, 9) suggest that volcanic rocks of the CKD are significantly different from any other rocks in the Kurile-Kamckatka arc, and form a separate (decoupled) field on any diagram. We also note that many of the across-arc trends reported in Dorendorf et al. (2000) and Churikova et al. (2001) are possibly related to this regional difference and may reflect the strikingly different

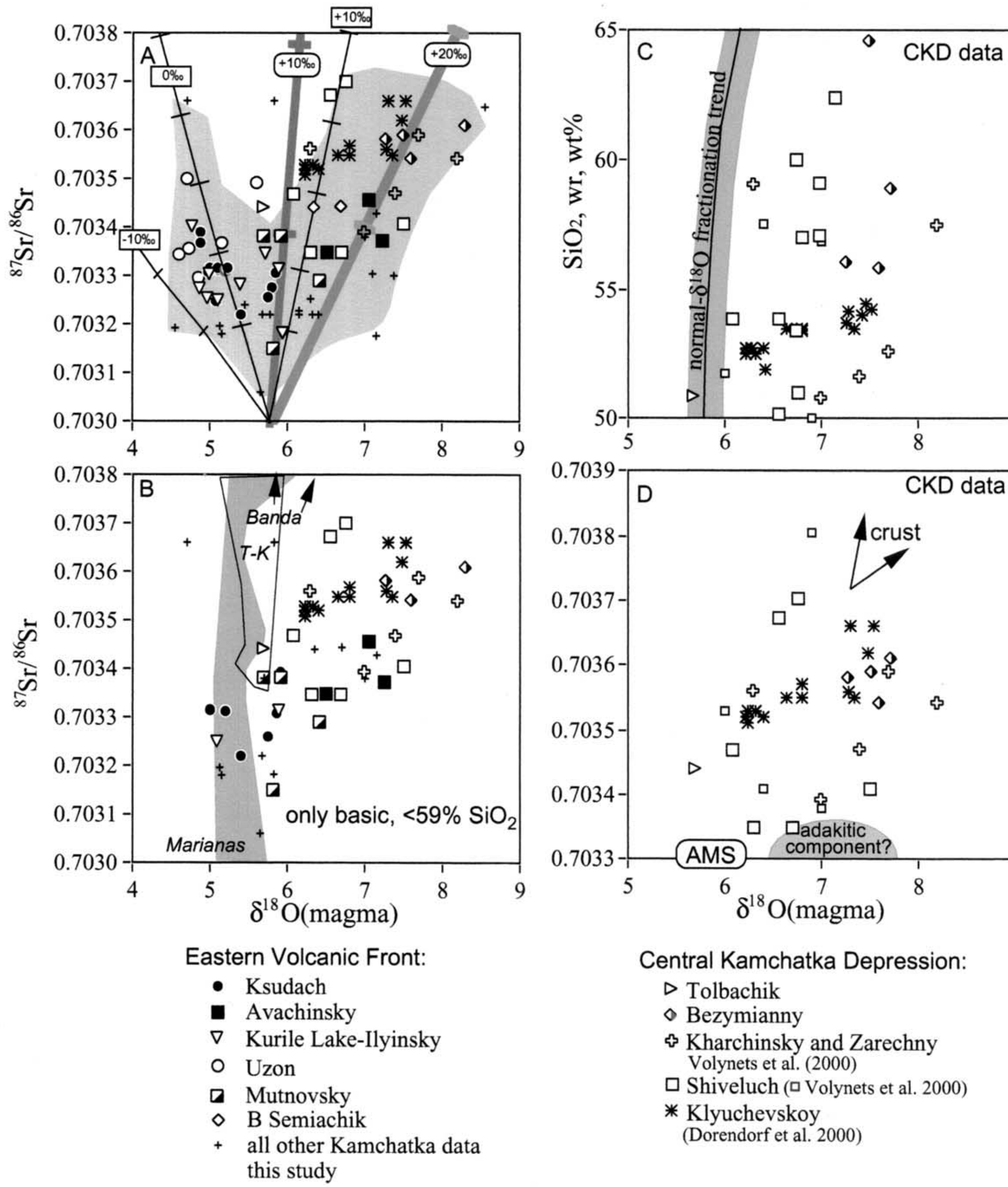

Fig. 8. $\delta^{18}O$(magma) vs. $^{87}Sr/^{86}Sr$ and SiO_2 correlations for Kamchatkan volcanic rocks; $\delta^{18}O$(magma) values are calculated from phenocrysts (see text and Table 1). (A) All data; notice V-shaped overall correlation: there is a negative correlation of $\delta^{18}O$(magma) vs. $^{87}Sr/^{86}Sr$ for low-$\delta^{18}O$ magmas from volcanoes of the EVF (Kurile Lake-Ilyinsky, Ksudach, and Uzon), and an overall positive correlation of $\delta^{18}O$(magma) vs. $^{87}Sr/^{86}Sr$ Kamchatka-wide from EVF to CKD. Mass balance curves for bulk mixing (tick marks are 5% increments) aim to model assimilation of low-$\delta^{18}O$ and high-$\delta^{18}O$ crusts, and addition of high-$\delta^{18}O$ fluids to magma generation zones. All fluids and assimilants have $^{87}Sr/^{86}Sr = 0.7045$; numbers in ovals are $\delta^{18}O$ for fluids, numbers in squares are for assimilants. The data is most consistent with derivation of both high- and low-$\delta^{18}O$ magmas from similar high-$\delta^{18}O$ and low-$\delta^{18}O$ crustal sources, rather than a source enrichment process; the latter would require an unrealistically high proportion (~10%) of fluid with $\delta^{18}O(\text{fluid}) = +20‰$, and low $^{87}Sr/^{86}Sr$ (ca. 0.704). See text for discussion. (B) Basic volcanic rocks (SiO_2 <59%). With few exceptions (see Table 1) basic rocks tend to form a positive trend towards high-$\delta^{18}O$ values; silicic rocks scatter and many have low-$\delta^{18}O$ magmatic values. This is in contrast with other circum Pacific arcs: Tonga-Kermadec (T-K, Bindeman, Turner et al., in prep) and Mariana arcs (shaded area, data are from fig. 3 of Eiler et al., 2000) (C, D) Rocks from the Central Kamchatka Depression (CKD, this work and published sources). Normal-$\delta^{18}O$ array for high-Mg basalt is from Figure 4. Notice initially high-$\delta^{18}O$ character of basic rocks and significant initial scatter in both $\delta^{18}O$ and $^{87}Sr/^{86}Sr$ isotopic ratios. Arrows in D aim to explain isotopic variation by mixing of lower crustal (from Fig. 3B), arc-mantle source (AMS), and a slab-melt adakitic component (low-Sr/Y, low $^{87}Sr/^{86}Sr$, high-Mg-andesite, e.g., Drummond et al., 1996).

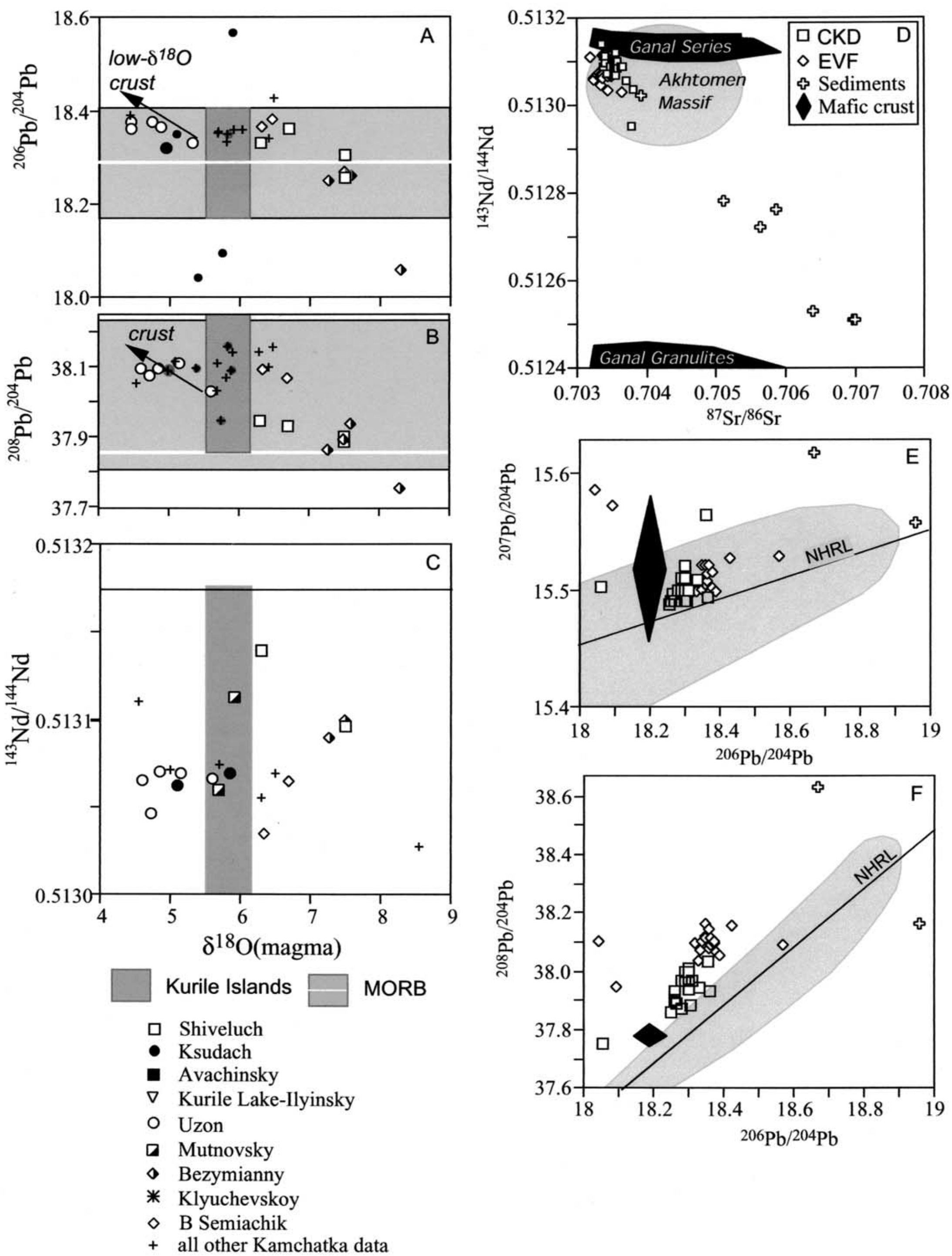

Fig. 9. Radiogenic isotopes of Nd and Pb vs. δ^{18}O(magma) (A–C). Data are from Tables 1 and 3. Note (A–C) rather primitive parameters for composition of other radiogenic isotope systems and subtle negative trends for Pb isotopes, as volcanoes in the CKD (Shiveluch, Bezymianny) tend to have lower values of $^{206}Pb/^{204}Pb$, and $^{208}Pb/^{204}Pb$. MORB and Kurile island arc volcanic rocks (data from Bindeman and Bailey, 1999) are shown for comparison; Kamchatka is characterized by more variable and higher $^{87}Sr/^{86}Sr$, but similar Pb and Nd isotopic ratios. D-F: $^{143}Nd/^{144}Nd$ vs. $^{87}Sr/^{86}Sr$, and $^{207}Pb/^{204}Pb$ vs. $^{206}Pb/^{204}Pb$, $^{208}Pb/^{204}Pb$ vs. $^{206}Pb/^{204}Pb$ diagrams showing differences between CKD and EVF volcanics, and potential mantle and crustal reservoirs that are capable of causing the isotopic variations. Sediment data is from this study (Table 4); crustal rocks are from Vinogradov (1995) and L'vov et al. (1986).

Table 4. Ocean floor materials in front of the Kamchatka trench.

Sample*	Iithology	$\delta^{18}O$, ‰	$^{87}Sr/^{86}Sr$	$^{143}Nd/^{144}Nd$	$^{206}Pb/^{204}Pb$	$^{207}Pb/^{204}Pb$	$^{208}Pb/^{204}Pb$
Dredged sediments							
V21-151	mud	10.41	0.70588	0.51276	18.668	15.616	38.627
RAMA-30-Bx	mud	11.47	0.70512	0.51278			
RAMA-31-PG	mud	13.19	0.70601				
RAMA-31-P	mud	11.05	0.70566	0.51272			
RAMA-44-P	mud	11.55	0.70698	0.51251			
RAMA-45-G	mud	11.73	0.70701	0.51251			
RAMA-32-G	mud	11.76	0.70641	0.51253			
DSDP 192							
192-32-2	clay	19.56	0.70786				
192-24-2	clay	17.90	0.70651				
192A-4-2	clay	21.31	0.70443				
192-20-1	diatom ooze	15.22	0.70624				
192-6-2	diatom ooze	16.74	0.70719				
192A-5-3	altered basalt	9.73	0.70393	0.51302	18.958	15.556	38.158
192-15-3	diatom ooze	23.35	0.70689				
192-6-2	diatom ooze	9.93	0.70402				

* See Bailey (1993, 1996) for sample description, and additional analyses of DSDP holes 193, 303, 304.

extensional tectonic regime and thinner crust in the CKD. Existing isotopic analyses of lower crustal rocks (Figs. 9D–F and 3B) are permissive end-members for derivation of basic to intermediate rocks through the interaction of arc mantle magma with the lower crust by a MASH-type process (e.g., Hildreth and Moorbath, 1988); this hypothesis is pending better support from Os isotopes in mafic volcanics.

5.4. Comparison with Other Island Arc Systems

A number of regional laser fluorination studies of O-isotopes in phenocrysts have recently been performed on other arcs (Thirlwall et al., 1996; McPherson et al., 1998; Eiler et al., 2000b; Vroon et al., 2001), and the results were correlated to radiogenic isotopes and trace elements. These studies considered both intraoceanic ensimatic (e.g., Marianas), and ensialic (e.g., Banda) arcs, but demonstrated only subtle magmatic $\delta^{18}O$ variations in magmas within normal-$\delta^{18}O$ range. Most previous whole-work studies erroneously overestimated the $\delta^{18}O$ enrichment as a result of the secondary low-T alteration. For example, Vroon et al. (2001) found only normal- to slightly high-$\delta^{18}O$ range of 5.5 to 6.5‰ in ensialic Banda arc, in sharp contrast to previous whole-rock studies that showed 5 to10‰ range (NB: there are no low-$\delta^{18}O$ magmas, i.e., $<$5.5‰, in the Banda arc). Unlike Kamchatka, narrow $\delta^{18}O$ range in Banda's volcanics, as well as even narrower $\delta^{18}O$ ranges in the Mariana and Tonga-Kermadec arcs (Fig. 8b), are coupled with significant range in radiogenic isotopes (e.g., $^{87}Sr/^{86}Sr = 0.7045$ to 710); these features at Banda arc are interpreted to largely represent contribution from subducted continental material. In most other arcs (e.g., Fig. 8b), the narrow and MORB-like phenocrysts-based $\delta^{18}O$ values were attributed to reflect 0.1–2% fluid $\pm$ sediments addition to the mantle wedge, negligibly affecting bulk $\delta^{18}O$. Where more sediments is subducted within a fracture zone, slightly elevated $\delta^{18}O$ values may result (e.g., 5.8–6.5‰ at Seguam island in the Aleutians, Singer et al., 1992). The discussion below presents compelling evidence for chiefly crustal origin of strong $\delta^{18}O$ variations in the Kamchatkan volcanic arc.

6. DISCUSSION

6.1. High-$\delta^{18}O$ Basic Rocks of Kamchatka

The widespread occurrence of high-$\delta^{18}O$ basalts and basaltic andesites in Kamchatka could be explained by: (1) arc mantle-like (+5.8‰) basaltic magmas subsequently undergoing moderate amounts of assimilation of high-$\delta^{18}O$ (ca. +10‰) supracrustal rocks in the lower or middle crust; (2) addition of high-$\delta^{18}O$ (ca. +10–20‰) slab fluids into magma generation zones; and (3) parental basic magmas with high-$\delta^{18}O$ of 6.5 to 7.2‰, derived by melting of the thickened lower crust.

In general, it is likely that all these sources variably contributed to the overall high-$\delta^{18}O$ signature. Either source (slab) or lower to midcrustal metamorphic wall rock assimilants are predominantly high-$\delta^{18}O$ rocks, and should lead to increasing $\delta^{18}O$ in magmas. The abundance of lower-crustal and mantle xenoliths in high-$\delta^{18}O$ volcanoes of CKD, and in Bakening and Avachinsky (EVF) (e.g., Widom et al., 2003) argues for a lower crustal to mantle-derived high-$\delta^{18}O$ signature. Widom et al. (2003) interpreted relatively radiogenic $^{187}Os/^{188}Os$ (0.123 to 0.157) in metasomatized peridotite xenoliths as evidence for multi-stage fluid addition to the arc mantle. Magma contamination by materials from the lower crust is supported by abundant and variously digested lower crustal amphibole-bearing xenoliths observed by us in Shiveluch, Bezymianny, and Avachinsky volcanoes; their host lavas tend to have high-$\delta^{18}O$ and $^{87}Sr/^{86}Sr$ (Fig. 9), similar to Mesozoic to Cenozoic lower-crustal xenoliths elsewhere (e.g., Ducea, 2002, and references therein). For siliceous rocks of Khangar volcano (and older volcanoes on the on the Sredinny Range), assimilation of high-$\delta^{18}O$ and $^{87}Sr/^{86}Sr$ crustal rocks is documented (Dril et al., 1999; Fig. 3A). This particular scenario should be constrained by detailed petrogenetic studies at each volcanic center. There is no unambiguous regional correlation of $\delta^{18}O$(magma) for basalt with distance from the trench, or with distance or position along the arc.

In discriminating between models 1–3 above, we have attempted to explain the mass balance of oxygen and Sr isotopes

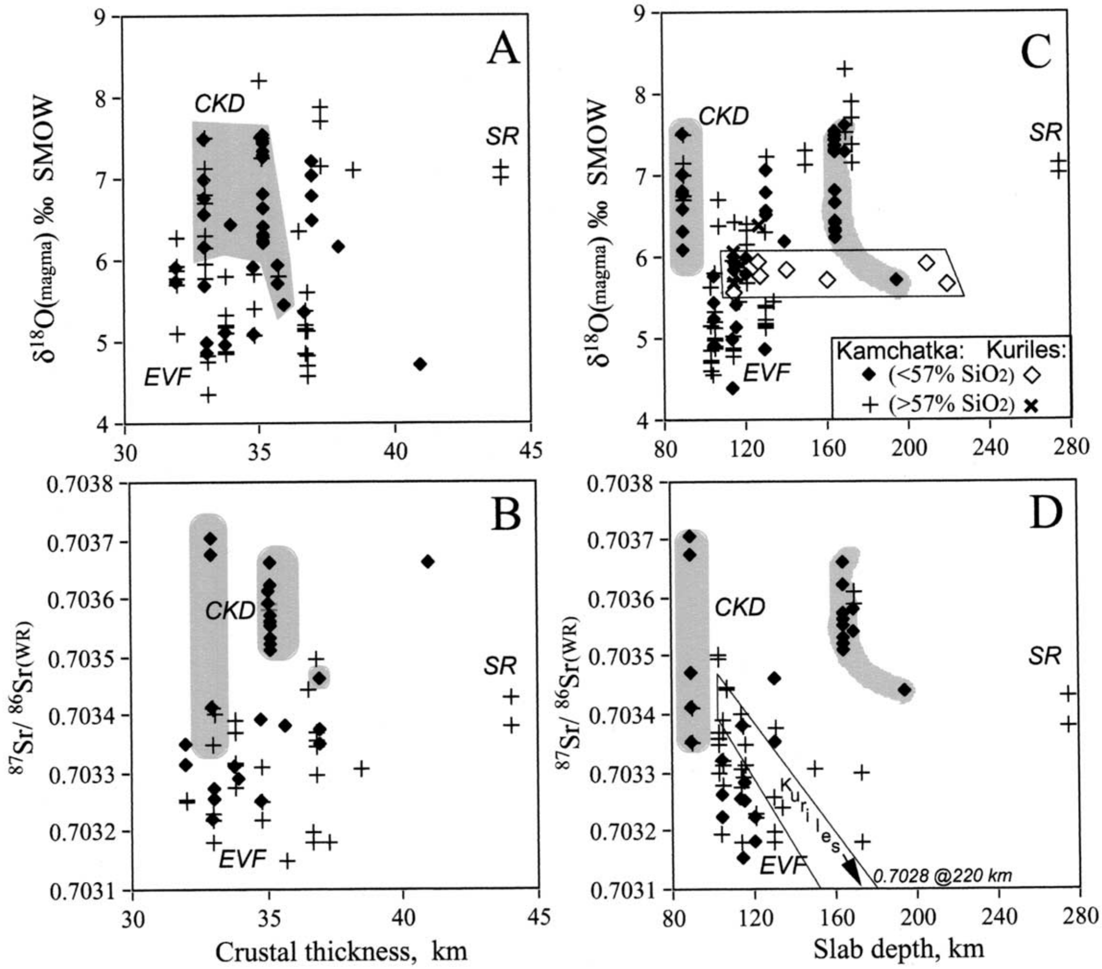

Fig. 10. Correlation of δ^{18}O(magma) and ^{87}Sr/^{86}Sr with (A, B) crustal thickness and (C, D) slab depth (crustal and subduction parameters are from Bogdanov and Khain, 2000) for Kamchatkan volcanic arc. Notice: (1) significant scatter at each slab depth and crustal thickness; (2) scattered positive correlations for mafic rocks from EVF to CKD and SR, and worse correlation for silicic rocks (A, C); (3) Greater slab depth correlates positively with increasing crustal thickness. The increasing ^{87}Sr/^{86}Sr with slab depth (D) is the opposite to of the Kurile island arc (sloped box, data from Bindeman and Bailey, 1999), a southern extension of the same subduction zone; there is no dependence of δ^{18}O(magma) on slab depth for the Kuriles. The S and O isotopes in Kamchatka are interpreted to represent greater source variability and crustal influence on the isotopic record (see text).

by performing simple bulk mixing calculations involving fluids and solid end-members with an expected range of values. Fluid contained 600 ppm Sr, 89% oxygen; assimilant and initial melt contained 200–500 ppm Sr and 50% oxygen; δ^{18}O(fluid or assimilant) = +10‰, 15‰, 20‰; ^{87}Sr/^{86}Sr = 0.703 (initial basalt), 0.7045 to 0.706 (assimilant or fluid), and δ^{18}O(upper crustal assimilant) were ranged from −15‰ to −5% and 0‰ (Fig. 8A). A bulk mixing model was chosen for simplicity since it provides minimum proportions for fluid or assimilant addition. Classical or energy-constrained AFC should yield (prohibitively) larger proportions of assimilant or fluid per mass of residual melt remaining.

Slab fluid addition into mantle magma sources (i.e., slab-induced melting) underneath each volcano (e.g., Dorendorf et al., 2000, for Kluychevskoy) with variable δ^{18}O(fluid) and ^{87}Sr/^{86}Sr(fluid) composition can match the isotopic composition of O and Sr in lavas only if excessive amounts (10–20 wt%) of fluids are involved. Additionally, such model fluid should have an extremely high-δ^{18}O (>+20‰) with very moderate ^{87}Sr/^{86}Sr = 0.704 (Fig. 8A). This is difficult to achieve from the altered oceanic crust (δ^{18}O = +2 to +10‰, Muehlenbachs, 1986), and is contrary to both δ^{18}O and ^{87}Sr/^{86}Sr values in sediments (Table 4) that are dominated by arc-derived clastic materials with an insignificant proportion of intraoceanic material. A carbonate-derived fluid (with δ^{18}O>25‰) would satisfy end-member restrictions, but no significant carbonate layers have been identified by dredging or drilling in the NW Pacific (Bailey, 1993, 1996; Prueher and Rea, 2001). The fluid derived from Kurile-Kamchatka trench sediments is expected to be higher in ^{87}Sr/^{86}Sr (>0.706) and lower in δ^{18}O (+8–10‰) than the required hypothetical end-member fluid.

Assimilation of crustal materials by mantle-equilibrated basaltic magmas would require high 20–40% assimilant addition

(Fig. 8B). If equal amounts of crystallization per mass of assimilant added are involved, these proportions are twice as high. Following the argument of Bindeman and Valley (2003), it would be even more difficult to achieve tens of percent assimilation when energy conservation (Spera and Bohrson, 2001) is considered. Thus, mass balance prohibits assimilation and, as with fluids, this process would be difficult to reconcile with the observed isotopic trends.

The simplest explanation of high-δ^{18}O in basic magmas (Fig. 8B), the rather primitive radiogenic isotopic signatures, and the observed V-shaped pattern of δ^{18}O(magma) vs. ^{87}Sr/^{86}Sr (Fig. 8A) is that of direct derivation of Kamchatkan magmas from parental sources that are high and variable in δ^{18}O. In this case magmas are formed by melting of older high-δ^{18}O, or low-δ^{18}O volcanic arc rocks with moderate ^{87}Sr/^{86}Sr and ^{206}Pb/^{204}Pb in a high heat flux environments. The recycling of older (Cretaceous to Cenozoic) volcanic materials (e.g., high-δ^{18}O hydrated metabasalts) provides a viable solution. High-δ^{18}O values in these sources could either be explained by long-term, deep-seated δ^{18}O-enrichment by slab fluids during various subduction configurations; or by low-temperature near-surface alteration, followed by burial by tectonic and magmatic processes. The range of $>$ 1‰ observed in olivines from Klyuchevskoy volcano by Dorendorf et al. (2000) is interpreted here to suggest derivation by mixing of (at least) two sources: an arc mantle source basalt, and high-δ^{18}O, high-^{87}Sr/^{86}Sr lower crustal melts. Large δ^{18}O and ^{87}Sr/^{86}Sr heterogeneity, and the adakitic trace elemental signature that is seen in other volcanoes of the CKD, and in Shiveluch in particular (Figs. 8C,D) would require an additional adakitic component (moderately high O and low Sr isotopes). No δ^{18}O characterization for adakite exists, but it is assumed here to be moderately elevated, since adakitic melts are thought to be derived from the hydrated slab ($\pm$ sediments) which tends to be high in δ^{18}O.

The majority of modern volcanic rocks in Kamchatka (Figs. 8, 9) are intermediate in SiO_2, whereas primitive basalts are rare in Kamchatka and in similar arcs built on thick crust (e.g., Andes; Hildreth and Moorbath, 1988). An origin of the dominant and voluminous magma types of basaltic andesites and andesites by crustal remelting can be plausibly driven by the heat of primitive basalts and high heat flux. Therefore, our preferred model for the majority of Kamchatkan basic magmas is that of recycling and remobilization of high-δ^{18}O Kamchatkan arc roots. Such a model of multi-stage enrichments, storage, tectonic and volcanic burial, and remelting is supported by the low level of Th-disequilibria in Kamchatkan volcanic rocks (Turner et al., 1998), which show absent or small (ca. "$<$150 k.y.") disequilibria, and do not exhibit significant Ra or ^{232}Th excesses. More significant U-Th disequilibria are seen in volcanoes of CKD (Dosseto and Bourdon, 2002) and suggests that mantle melting, assimilation and mixing were sufficiently rapid (e.g., $<$100 k.y.); we speculate that some of the U-Th disequilibria may have been generated during devolatilization melting of lower crustal amphibole-bearing metabasalts underplated by hot mantle-derived magmas (e.g., Rapp and Watson, 1995). Slab detachment beneath CKD (e.g., Levin et al., 2003) may cause rather rapid upwelling of deep hot mantle and interaction with the mafic arc roots, yielding voluminous volcanism, some with intraplate affinity. Additionally, recent treatments of thermal regime in the convecting mantle wedge are more consistent with $>$100°C hotter subarc mantle than previously thought (Kelemen et al., 2002). Geophysical data on crustal structure under CKD volcanoes (Fedotov and Masurenkov, 1991) are consistent with a significant (ca. 10 km) transition zone near the Moho which can be interpreted as remobilized arc roots.

6.2. Large-Scale ^{18}O Depletion of Kamchatkan Crust and Low-δ^{18}O Magmas

The outstanding result of the present study is the discovery that Kamchatka has a great abundance of low-δ^{18}O magmas, comparable only to Iceland. Low-δ^{18}O magmas bear evidence of magma interaction (through assimilation or bulk melting) with even stronger ^{18}O-depleted upper crustal country rocks. Accordingly, δ^{18}O values in low-δ^{18}O magmas serve as an upper estimate of crustal δ^{18}O values. Assimilation is viewed as melting of country rocks followed by mixing with the main differentiating magma reservoir.

The inferred degree of assimilation or melting is dependent on the average δ^{18}O value of the wall rocks, and this is a largely unknown parameter. For example, *if* the assimilation proportion were independently constrained at 20%, then the wall-rock (Kamchatkan crust) has -5 to -10‰ (e.g., Fig. 8D), but is equal to the assimilant if magmas are derived by bulk melting.

Hydrothermally-altered rocks were analyzed from surface exposures and boreholes of modern geothermal systems (Taran et al., 1988; Zolotarev et al., 1999) and yielded low δ^{18}O values down to -1‰. The δ^{18}O values of hydrothermally-altered rocks in a 1500 m deep drillhole through the modern Mutnovsky geothermal system (100–300°C) indicate a moderate level of depletion down to 0–3‰ (Taran et al., 1988), in equilibrium with moderately low values of -10 to -14‰ in present-day meteoric waters (Cheshko, 1994). However, most potential assimilants for genesis of Pleistocene and early Holocene low-δ^{18}O magmas have been affected by older fossil hydrothermal systems. In the latter, the level of ^{18}O-depletion is stronger, since these rocks interacted with extremely light (<-25‰) Pleistocene glacial melt waters, and presumably the geothermal systems died out or were quenched by glaciers during the Pleistocene. Rocks in equilibrium with these waters may be variably depleted down to -15‰, and δ^{18}O-depletion of 2‰ in a magma would require only a moderate ($<$10–20%) amount of assimilation.

Subtle negative correlation of δ^{18}O with radiogenic isotopes of Sr (and Pb, Figs. 8A, 9B,C) supports shallow recycling of older (Quaternary and older Cenozoic) and slightly more radiogenic material. The latter is likely due to both build up of radiogenic Sr due to aging effects in low-δ^{18}O crust, as well as leaching, transport, and addition of radiogenic Sr by circulating hydro thermal solutions from older and more radiogenic crustal rocks (^{87}Sr/^{86}Sr = 0.706–0.710, Fig. 3B) since low-δ^{18}O geothermal waters tend to be high in ^{87}Sr/^{86}Sr (Vinogradov and Vakin, 1983).

6.3. Climate Influence on Magma Sources?

Climate modeling studies suggest a wetter and colder climate for the NW Pacific in the Pleistocene (Jouzel et al., 1994; Kutzbach et al., 1998), in agreement with the palynological record on land (Braitseva et al., 1968) and in sediments (Ber-

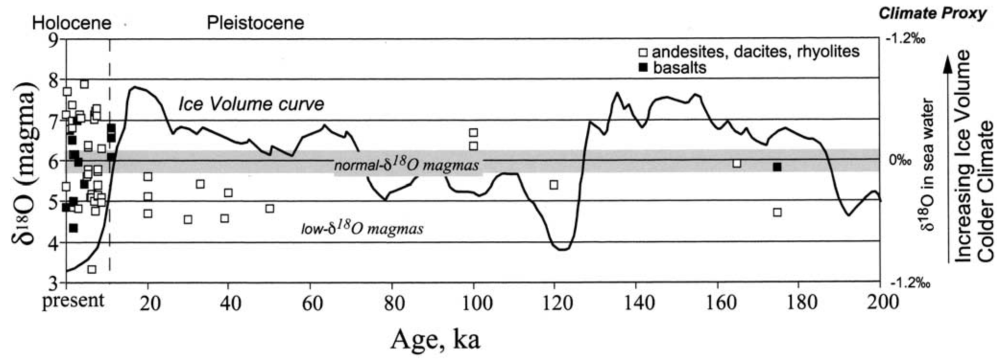

Fig. 11. Primary $\delta^{18}O$(magma) values (calculated from phenocrysts) plotted against age of eruption for Kamchatka. The lower $\delta^{18}O$ values for Pleistocene likely reflect assimilation of wall rocks that have interacted with low-$\delta^{18}O$ glacial meltwaters. Holocene volcanics show a larger scatter and trend towards higher values, because Holocene magmas assimilated both Pleistocene (low-$\delta^{18}O$) and Holocene (higher-$\delta^{18}O$) crust. Age on Pleistocene volcanic units is either determined by fission tracks in apatite, short-lived magnetic reversals, or geological data (compiled after Sheymovich, 1979; Melekestsev et al., 1988; Grib and Leonov, 1993a,b; Leonov and Grib, 1998; V. L. Leonov, personal communication); uncertainty on >20 ka volcanics is large and their ages relative to glacial/interglacial are not yet certain. Ice Volume curve (solid line) is from Bradley (2000).

ingia Drilling Project, 2001). Lower sea level stands created conditions for glaciations downwind (inland) on the eastern and south-eastern margins of north Pacific arcs (Mann and Peteet, 1994). Collectively, higher precipitation levels, colder climate, and rainout effects behind glaciers promoted voluminous precipitation of low-$\delta^{18}O$ and low-δD meteoric water inland in Kamchatka. The exact isotopic values during the Pleistocene were likely to vary temporally and laterally, but on average they were substantially lower than today. The $\delta^{18}O$ values of precipitation were likely below −25‰ during the last glaciation, by comparison with other glaciated areas (e.g., Dansgaard et al., 1993). Although the continental ice sheet during the last glaciation in Kamchatka is being dabated (e.g., Grosswald, 1998), voluminous and interconnected alpine glaciers which survived from winter to winter would be enough to yield ultra-low (ca. <−35‰) $\delta^{18}O$ snow meltwaters and cause a regional low-$\delta^{18}O$ fingerprint in rocks and magmas. The abundant low-$\delta^{18}O$ magmas provide a record of this widespread ^{18}O depletion of the upper crust in Kamchatka, and can be attributed to climate change during Pleistocene-Holocene. The ultra-low $\delta^{18}O$ meteoric waters that originated from these glaciers fed the geothermal systems and imparted a regional low-$\delta^{18}O$ fingerprint to rocks and magmas and thereby affected $\delta^{18}O$ and $^{87}Sr/^{86}Sr$ values of recent volcanic rocks. There has been a single report of exceptionally low-$\delta^{18}O$ (−28‰), and low-δD (−130‰) waters encountered in the borehole near Mutnovsky volcano (Pokrovsky, 2001). Such low values are lower than $\delta^{18}O$ in the present Kamchatkan glaciers (ca. −20) and, if not the result of complex underground evaporation-distillation processes, they might represent glacial water that has survived from the last glacial maximum.

When plotted against age (Fig. 11), primary magmatic $\delta^{18}O$ values show a significant range in the Holocene, but are generally low in $\delta^{18}O$ for the Pleistocene. Low-$\delta^{18}O$ values in Pleistocene magmas can be attributed to lower $\delta^{18}O$ values of meteoric waters and associated hydrothermal systems. Normal to high-$\delta^{18}O$ values of Holocene magmas reflect new magmas that did not interact with either Pleistocene or Holocene low-$\delta^{18}O$ crust. The persisting and abundant low-$\delta^{18}O$ magmas of the Holocene record a "memory" effect of >2 m.y.-long Pleistocene glaciation: many Holocene magmas could be derived from synglacially altered crust, or reflect its assimilation.

The great abundance (by number of volcanic units and their total volume) of low-$\delta^{18}O$ magmas in Kamchatka can be compared to the Pleistocene-Holocene record in Iceland. Kamchatka was the second most volcanically active subaerial region during the Holocene (Simkin and Siebert, 1994); high endogenic heat flux, and ^{18}O-depleted waters are responsible for the large-scale depletion of the upper crust of Kamchatka (and Iceland) with respect to ^{18}O. Widespread ^{18}O-depleted areas are described from Mesozoic terrains and attributed to their subpolar location (e.g., Blattner et al., 1997). Identification of the large Late Cenozoic province of Kamchatka is a significant discovery which can serve as a model province for the interpretation of past $\delta^{18}O$ records preserved in rocks. We suggest that earlier colder periods in the Earth's history (e.g., Rumble and Yui, 1998) such as the "snowball Earth," when moderately low-$\delta^{18}O$ glaciers covered the surfaces of entire land-masses at low latitudes, as well as the subpolar position of some continents (with ultra-low-$\delta^{18}O$ glaciers) at certain geologic periods, can be inferred from the abundance of low-$\delta^{18}O$ magmas both regionally and world-wide.

6.4. Implications for Other Convergent Margins

We were able to achieve discrimination of crustal vs. mantle processes in Kamchatka, largely because of the oxygen isotopic diversity of Kamchatkan magmas, possibly fingerprinted by the effect of the last glaciation. In lower latitude arcs, oxygen isotopic variations were shown to be more subdued (e.g., Baker et al., 1996; Eiler et al., 2000b; Vroon et al., 2001; our unpublished data for Tonga-Kermadec), as the isotopic contrast between $\delta^{18}O$ of Pleistocene precipitation and $\delta^{18}O$(magma) was less severe. The torque of oxygen isotope geochemistry is thus less powerful. Only in Alaska-Aleutian arc is there a comparable, but smaller range in $\delta^{18}O$ values in magmas (4.5 to

6.2‰, Singer et al., 1992; Bindeman et al., 2001); more synglacial volcanoes/calderas need to be sampled there. Nonetheless, similar processes of shallow and deep recycling are likely to be characteristic for other, lower latitude arcs, but the isotopic effect on magmas may not be currently analytically detectable. In this respect Kamchatka represents the best example ("natural laboratory") to clearly demonstrate such processes. The large-scale low-$\delta^{18}O$ anomaly in the upper crust of Kamchatka contradicts earlier reports that the measured D/H, $^{18}O/^{16}O$, and $^{87}Sr/^{86}Sr$ ratios in volcanics and their phenocrysts in many Kamchatkan volcanoes directly reflect those in the mantle (e.g., Volynets, 1994; Taran et al., 1997; Pineau et al., 1999; Pokrovsky and Volynets, 1999; Churikova et al., 2001). The difference in $\delta^{18}O$ values in differentiated volcanics between neighboring calderas may reach 3‰ (e.g., Uzon vs. Bolshoi Semiachik, Table 2) and, as we have shown above, is due to near-surface processes. The $\delta^{18}O$ and δD values of modern fumarolic and geothermal waters in Kamchatka are generally lower than in the neighboring Kurile islands (Giggenbach, 1992; Cheshko, 1994; Taran et al., 1997; Fisher et al., 1998), which is consistent with latitudinal and altitudinal effects on meteoric water precipitation, and on a shallow rather than deep origin of $\delta^{18}O$ and δD variations.

We presented arguments above that both high- and low-$\delta^{18}O$ signatures are of crustal origin and best explained by lower- and upper- crustal processes, respectively. This study, based on $\delta^{18}O$, also suggests the indirect influence of climate on isotopic signatures of volcanism, and demonstrates the importance of recycling older arc-derived crustal materials in recent postglacial volcanism; this has significant implications for lithosphere-scale oxygen isotope stratification in modern and ancient convergent margins, in newly created (Iceland) and newly accreted (Kamchatka) lithospheres.

Acknowledgments—The results of this work were made possible by the decade-long field efforts of the authors. We are grateful to O. A. Braitseva, B. G. Pokrovsky, O. B. Selyangin, M. M. Pevzner, T. I. Frolova, I. A. Burikova, V. L. Leonov, E. N. Grib, P. Izbekov, Philip Kyle and Peter Rinkleff for sample donation and discussion. Several important samples studied in this paper originally came from the collections of the late O. N. Volynets, handled by A. B. Perepelov. Discussions with John Fournelle on the Aleutians helped us with this Kamchatka study; early work by V. I. Vinogradov in Kamchatka provoked many of the interpretations favored here. Mike Spicuzza is thanked for assistance in stable isotope analyses. Comments and reviews by Chris Harris, Greg Holk, Maxim Portnyagin, Bill Leeman, Simon Sheppard, and an anonymous reviewer are greatly appreciated. We thank DOE (93ER14389) for funding the oxygen isotope research. Field work was funded by grants 6215–98 and 6543–99 from the National Geographic Society and by the Russian Foundation for Basic Research.

Associate editor: S. M. F. Sheppard

REFERENCES

Anderson A. T., Clayton R. N., and Mayeda T. (1971) Oxygen isotope thermometry of mafic igneous rocks. *J. Geol.* **79,** 714–729.

Appora I., Eiler J. M., Matthews A., and Stolper E. M. (2003) Experimental determination of oxygen isotope fractionations between CO_2 vapor and soda-melilite melt. *Geochim. Cosmochim. Acta* **67,** 459–471.

Bailey J. C. (1996) Role of subducted sediments in the genesis of Kurile-Kamchatka island arc basalts: Sr isotopic and elemental evidence. *Geochem. J.* **30,** 289–321.

Bailey J. C. (1993) Geochemical history of sediments in the northwestern Pacific Ocean. *Geochem. J.* **27,** 71–91.

Bailey J. C., Larsen O., and Frolova T. I. (1987) Strontium isotope variations in Lower Tertiary-Quaternary volcanic rocks from the Kurile island arc. *Contrib. Mineral. Petrol.* **95,** 155–165.

Baker J. A., Macpherson C. G., Menzies M. A., Thirlwall M. F., Al-Kadasi M., and Mattey D. P. (2000) Resolving crustal and mantle contributions to continental flood volcanism, Yemen: Constraints from mineral isotope data. *J. Petrol.* **41,** 1808–1820.

Baranov B. V., Seliversov N. I., Muraviev A. V., and Mazurov E. L. (1991) The Kommandorsky Basin as a product of spreading behind a transform plate boundary. *Tectonophysics* **99,** 237–269.

Beget J. E. (2001) Continuous Late Quaternary proxy climate records from loess in Beringia. *Quat. Sci. Rev.* **20,** 499–507.

Beringia Drilling Project. (2001) Holocene paleoclimate data from the Arctic: Testing models of global climate change. *Quat. Sci. Rev*. **20,** 1275–1287.

Bindeman I. N. and Bailey J. C. (1994) A model of reverse differentiation at Dikii Greben' Volcano, Kamchatka: Progressive basic magma vesiculation in a silicic magma chamber. *Contrib. Mineral. Petrol.* **117,** 263–278.

Bindeman I. N. and Bailey J. C. (1999) Trace elements in anorthite megacrysts from the Kurile island arc: A window to across-arc geochemical variations in magma compositions. *Earth Planet. Sci. Lett.* **169,** 209–226.

Bindeman I. N., Fournelle J. H., and Valley J. W. (2001) 9100 BP Eruption of Fisher Caldera, Unimak, Aleutians: Low-$\delta^{18}O$ zoned tuff, a tephrochronological marker. *J. Volc. Geotherm. Res.* **111,** 35–53.

Bindeman I. N., Vinogradov V. I., Valley J. W., Wooden J. L., and Natalin B. A. (2002) Archean protolith, and accretion of crust in Kamchatka: SHRIMP dating of zircons from metamorphic rocks of Sredinny and Ganal Massifs. *J. Geol.* **110,** 271–289.

Bindeman I. N. and Valley J. W. (2003) Rapid generation of both high- and low-$\delta^{18}O$, large volume silicic magmas at the Timber Mountain/Oasis Valley caldera complex, Nevada. *Geol. Soc. Am. Bull.* **115,** 581–595.

Blattner P., Grindley G. W., and Adams C. J. (1997) Low-^{18}O terranes tracking Mesozoic polar climates in the South Pacific. *Geochim. Cosmochim. Acta* **61,** 569–576.

Bogdanov N. A. and Khain V. E. (eds.) (2000) Tectonic map of the Sea of Okhotsk region. Explanatory notes. Scale 1:2,500,000. Nedra.

Bradley R. S. (2000) *Paleoclimatology: Reconstructing Climates of the Quaternary* 2nd ed. Academic.

Braitseva O. A., Melekestsev I. V., Evteeva I. C., and Lupikina E. G. (1968) *Stratigraphy of Quaternary deposits and glaciations of Kamchatka*. (in Russian).Nauka.

Braitseva O. A., Litasova S. N., and Ponomarenko A. K. (1987) Application of tephrochronological method for dating of the key archaeological site in Eastern Kamchatka. *Volcanol. Seismol.* **5/5,** 507–514.

Braitseva O. A. and Melekestsev I. V. (1990) Eruptive history of Karymsky volcano, Kamchatka, USSR, based on tephra stratigraphy and ^{14}C dating. *Bull. Volcanol.* **53,** 195–206.

Braitseva O. A., Melekestsev I. V., Ponomareva V. V., and Sulerzhitsky L. D. (1995) The ages of calderas, large explosive craters and active volcanoes in the Kuril-Kamchatka region, Russia. *Bull. Volcanol.* **57/6,** 383–402.

Braitseva O. A., Melekestsev I. V., Ponomareva V. V., and Kirianov V. Y. (1996) The caldera-forming eruption of Ksudach volcano about AD 240, the greatest explosive event of our era in Kamchatka. *J. Volcanol. Geotherm. Res.* **70,** 49–66.

Braitseva O. A., Ponomareva V. V., Sulerzhitsky L. D., Melekestsev I. V., and Bailey J. C. (1997a) Holocene key-marker tephra layers in Kamchatka, Russia. *Quat. Res.* **47,** 125–139.

Braitseva O. A., Sulerzhitsky L. D., Ponomareva V. V., and Melekestsev I. V. (1997b) Geochronology of the greatest Holocene explosive eruptions in Kamchatka and their imprint on the Greenland glacier shield. *Trans. (Doklady) Russian Acad. Sci. Earth Sci. Sect.* **352,** 138–140.

Brigham-Grette J. (2001) New perspectives on Beringian Quaternary paleogeography, stratigraphy, and glacial history. *Quat. Sci. Rev.* **20,** 15–24.

Chacko T., Cole D. R., and Horita J. (2001) Equilibrium oxygen, hydrogen, and carbon isotope fractionation factors: Applicable to geologic systems. *Rev. Mineral. Geochem.* **43,** 1–82.

Cheshko A. L. (1994) D, $^{18}O/^{16}O$, and $^{3}He/^{4}He$ data on the formation of the main types of thermal waters in the Kurile-Kamchatka region. *Geochem. Int.* **32,** 988–1001.

Chiba H., Chacko T., Clayton R. N., and Goldsmith J. R. (1989) Oxygen isotope fractionations involving diopside, forsterite, magnetite and calcite; application to geothermometry. *Geochim. Cosmochim. Acta* **53,** 2985–2995.

Churikova T., Dorendorf F., and Woerner G. (2001) Sources and fluids in the mantle wedge below Kamchatka, evidence from across-arc geochemical variation. *J. Petrol.* **42,** 1567–1593.

Condomines M., Gronvold K., Hooker P. J., Muehlenbachs K., O'Nions R. K., Oskarsson N., and Oxburgh E. R. (1983) Helium, oxygen, strontium and neodymium isotopic relationships in Icelandic volcanics. *Earth Planet. Sci. Lett.* **66,** 125–136.

Dansgaard W., Johnsen S. J., Clausen H. B., Dahljensen D., Gundestrup N. S., Hammer C. U., Hvidberg C. S., Steffensen J. P., Sveinbjornsdottir A. E., Jouzel J., and Bond G. (1993) Evidence for general instability of past climate from a 250-kyr ice-core record. *Nature* **364,** 218–220.

Davidson J. P. (1989) Crustal contamination vs. subduction zone enrichment: Examples from the Lesser Antilles and implications for the mantle source composition of island arc volcanic rocks. *Geochim. Cosmochim. Acta* **51,** 2185–2198.

Donnely-Nolan J. M. (1998) Abrupt shift in delta ^{18}O values at Medicine Lake volcano (California, USA). *Bull. Volcanol.* **59,** 529–536.

Dorendorf F., Wiechert U., and Worner G. (2000) Hydrated sub-arc mantle: A source for the Kluchevskoy volcano, Kamchatka/Russia. *Earth Planet. Sci. Lett.* **175,** 69–86.

Dosseto A. and Bourdon B. (2002) Models for genesis of Kamchatka arc magmas: New insights from U-series (abstract). *Geochim. Cosmochim. Acta* **66***(15A),* A193–A193.

Dril S. I., Pokrovsky B. G., Perepelov A. B., Baluyev E. Y. and Bankovskaya E. V. (1999) Khangar Volcano (Kamchatka): $^{87}Sr/^{86}Sr$-$\delta^{18}O$ isotope systematics and genesis of lavas. In *Proceedings of the International Conference on Isotope Geochemistry*, p. 124. Moscow. Vernadsky Institute (Abstr.).

Drummond M. S., Defant M. J., and Kepezhinskas P. K. (1996) Petrogenesis of slab-derived trondhjemite-tonalite-dacite/adakite magmas. *Trans. R. Soc. Edinburgh* **87,** 205–215.

Ducea M. N. (2002) Constraints on the bulk composition and root foundering rates of continental arcs: A California arc perspective. *J. Geophys. Res.* **107***(B11),* 2304.

Eiler J. M. (2001) Oxygen isotope variations in basaltic lavas and upper mantle rocks. *Rev. Mineral. Geochem.* **43,** 319–364.

Eiler J. M., Gronvold K., and Kitchen N. (2000a) Oxygen isotope evidence for the origin of chemical variations in lavas from the Theistareykir volcano in Iceland's northern volcanic zone. *Earth Planet. Sci. Lett.* **184,** 269–286.

Eiler J. M., Crawford A., Elliott T., Farley K. A., Valley J. W., and Stolper E. M. (2000b) Oxygen isotope geochemistry of oceanic-arc lavas. *J. Petrol.* **41,** 229–256.

Engebretson D. C., Cox A. and Gordon R. G. (1985) Relative motions between oceanic and continental plates in the Pacific basin. Special Paper 206. Geol. Soc. Am.

Erlich E. (1986) Geology of the calderas of Kamchatka and Kurile islands with comparison to calderas of Japan and the Aleutians, Alaska. Open File Report 86-291. U.S. Geological Survey.

Fedotov S. A. and Masurenkov Yu. P. (eds.) *Active Volcanoes of Kamchatka. (*1991) 2 vols. Nauka.

Fisher T. P., Giggenbach W. F., Sano Y., and Williams S. N. (1998) Fluxes of volatiles discharged from Kudriavy, a subduction zone volcano, Kurile Islands. *Earth Planet. Sci. Lett.* **160,** 81–96.

Gautason B. and Muehlenbachs K. (1998) Oxygen isotopic fluxes associated with high-temperature processes in the rift zones of Iceland. *Chem. Geol.* **145,** 275–286.

Geist E. L., Vallier T. L., and Scholl D. W. (1994) Origin, transport and emplacement of exotic island arc terranes exposed in eastern Kamchatka, Russia. *Geol. Soc. Am. Bull.* **106,** 1182–1194.

Ghiorso M. S. and Sack R. O. (1995) Chemical mass-transfer in magmatic processes IV: A revised and internally-consistent thermodynamic model for the interpolation and extrapolation of liquid-solid equilibria at elevated temperatures and pressure. *Contrib. Mineral. Petrol.* **119,** 197–212 .

Giggenbach W. F. (1992) Isotopic shifts in waters from geothermal and volcanic systems along convergent plate boundaries and their origin. *Earth Planet. Sci. Lett.* **113,** 495–510.

Gill J. B. (1981) Orogenic Andesites and Plate Tectonics. Springer-Verlag.

Gorbatov A., Fukao Y., Widiyantoro S., and Gordeev E. (2001) Seismic evidence for a mantle plume oceanward of the Kamchatka-Aleutian trench junction. *Geophys. J. Int.* **146,** 282–288.

Grib E. N. and Leonov V. L. (1993a) Ignimbrites of the Bolshoi Semiachik caldera, Kamchatka: Composition, structure and origin. *Volcanol. Seismol.* **14,** 532–550.

Grib E. N. and Leonov V. L. (1993b) Ignimbrites of Uzon-Geyzernaya volcano-tectonic depression, Kamchatka: Correlation of sections, compositions and conditions of formation. *Volcanol. Seismol.* **14,** 15–33.

Grosswald M. G. (1998) Late-Weichselian ice sheets in Arctic and Pacific Siberia. *Quat. Int.* **45,** 3–18.

Gualtieri L., Glushkova O., and Brigham-Grette J. (2001) Evidence for restricted ice extent during the last glacial maximum in the Koryak Mountains of Chukotka, Far Eastern Russia. *Geol. Soc. Am. Bull.* **112,** 1106–1118.

Harris C., Smith H. S., and le Roex A. P. (2000) Oxygen isotope composition of phenocrysts from Tristan da Cunha and Gough Island lavas: Variation with fractional crystallization and evidence for assimilation. *Contrib. Mineral. Petrol.* **138,** 164–175.

Hattori K. and Muehlenbachs K. (1982) Oxygen isotope ratios of the Icelandic crust. *J. Geophys. Res.* **87,** 6559–6565.

Hemond C., Condomines M., Fourcade S., Allègre C. J., Oskarsson N., and Javoy M. (1988) Thorium, strontium and oxygen isotopic geochemistry in recent tholeiites from Iceland: Crustal influence on mantle-derived magmas. *Earth Planet. Sci. Lett.* **87,** 273–285.

Hildreth W. and Moorbath S. (1988) Crustal contribution to arc magmatism in the Andes of Central Chile. *Contrib. Mineral. Petrol.* **98,** 455–489.

Hochstaedter A. G., Kepezhinskas P., and Defant M. (1996) Insights into the volcanic arc mantle wedge from magnesian lavas from the Kamchatka arc. *J. Geophys. Res.* **101,** 697–712.

Hoefs J. (1997) Stable Isotope Geochemistry 4th ed. Springer-Verlag.

Ishikawa T., Tera F., and Nakazawa T. (2001) Boron isotope and trace element systemetics of the three volcanic zones in the Kamchatka arc. *Geochim. Cosmochim. Acta* **65,** 4523–4537.

Ivanov B. V. (1990) *Types of Andesite Volcanism in the Pacific Volcanic Belt* (in Russian). Nauka.

Izbekov P. E., Eichelberger J. C., Patino L. C., Vogel T. A., and Ivanov B. V. (2002) Calcic cores of plagioclase phenocrysts in andesite from Karymsky volcano: Evidence for rapid introduction by basaltic replenishment. *Geology* **30,** 799–802.

Jouzel J., Koster R. D., Suozzo R. J., and Russell G. L. (1994) Stable water isotope behavior during the last glacial maximum—A general-circulation model analysis. *J. Geophys. Res. Atm.* **99,** 25791–25801.

Kalamarides R. I. (1984) Kiglapait geochemistry VI: Oxygen isotopes. *Geochim. Cosmochim. Acta* **48,** 1827–1836.

Kelemen P., Parmentier M., Rilling J., Meh L., and Hacker B. (2002) Thermal convection of the mantle wedge. *Geochim. Cosmochim. Acta* **66***(15A),* A389–A389.

Kepezhinskas P., Defant M. J., and Drummond M. S. (1996) Progressive enrichment of island arc mantle by melt-peridotite interaction inferred from Kamchatka xenoliths. *Geochim. Cosmochim. Acta* **60,** 1217–1229.

Kepezhinskas P., McDermott F., Defant M. J., et al.. (1997) Trace element and Sr-Nd-Pb isotopic constraints on a three-component model of Kamchatka arc petrogenesis. *Geochim. Cosmochim. Acta* **61,** 577–600.

Kersting A. B. and Arculus R. J. (1994) Klyuchevskoi volcano, Kamchatka, Russia: The role of high flux, recharged, tapped and fractionated magma chamber(s) in the genesis of high Al_2O_3 from high MgO basalt. *J. Petrol.* **35,** 1–42.

Kersting A. B. and Arculus R. J. (1995) Pb isotopic composition of Klyuchevskoy volcano, Kamchatka and north Pacific sediments: Implications for magma genesis and crustal recycling in the Kamchatka arc. *Earth Planet. Sci. Lett.* **136,** 133–148.

Kohn M. J. and Valley J. W. (1998) Oxygen isotope geochemistry of the amphiboles: Isotope effects of cation substitutions in minerals. *Geochim. Cosmochim. Acta* **62,** 1947–1958.

Konstantinovskaya E. A. (2000) Geodynamics of an Early Eocene arc-continent collision reconstructed from Kamchatka Orogenic Belt, NE Russia. *Tectonophysics* **325,** 87–105.

Kutzbach J., Gallimore R., Harrison S., Behling P., Selin R., and Laarif F. (1998) Climate and biome simulations for the past 21,000 years. *Quat. Sci. Rev.* **17,** 473–506.

Leeman W. P. (1996) Boron and other fluid-mobile elements in volcanic arc lavas: Implications for subduction processes. In *Subduction: Top to Bottom*. Geophysics Monograph 96, pp. 269–276. American Geophysics Union.

Leonov V. L. and Grib E. N. (1998) Calderas and ignimbrites of Uzon-Semiachik area, Kamchatka. *Volcanol. Seismol.* **3,** 41–59.

Levin V., Shapiro N., Park J., and Ritzwoller M. (2003) Seismic evidence for catastrophic slab loss beneath Kamchatka. *Nature* **418,** 763–767.

Lvov A. B., Neelov A. N., Bogomolov E. S., and Mikhailova N. S. (1985) On the age of metamorphic rocks from Ganalsky Range, Kamchatka. *Geologia I Geophysika* **7,** 47–56.

Macias J. L. and Sheridan M. F. (1995) Products of 1907 eruption of Shtubel volcano, Ksudach caldera, Kamchatka, Russia. *Geol. Soc. Am. Bull.* **107,** 969–986.

Macpherson C. G., Gamble J. A., and Mattey D. P. (1998) Oxygen isotope geochemistry of lavas from an oceanic to continental arc transition, Kermadec-Hikurangi margin, SW Pacific. *Earth Planet. Sci. Lett.* **160,** 609–621.

Mann D. H. and Peteet D. M. (1994) Extent and timing of the last glacial maximum in SW Alaska. *Quat. Res.* **42,** 136–148.

Matsuhisa Y. (1979) Oxygen isotopic compositions of volcanic rocks from the east Japan island arc and their bearing on petrogenesis. *J. Volcanol. Geotherm. Res.* **5,** 271–296.

Matsuhisa Y., Matsubaya O., and Sakai H. (1973) Oxygen isotope variations in magmatic differentiation processes of the volcanic rocks in Japan. *Contrib. Min. Petrol.* **39,** 277–288.

Matthews A., Goldsmith J. R., and Clayton R. N. (1983) Oxygen isotope fractionations involving pyroxenes: The calibration of mineral pair geothermometers. *Geochim. Cosmochim. Acta* **47,** 631–644.

Matthews A., Palin J. M., Epstein S., Stolper and E. M. (1994) Experimental study of $^{18}O/^{16}O$ partitioning between crystalline albite, albitic glass and CO_2 gas. *Geochim. Cosmochim. Acta* **58,** 5255–5266.

Matthews A., Stolper E. M., Eiler J. M. and Epstein S. (1998) Oxygen isotope fractionation among melts, minerals and rocks. In *Proceedings of the 1998 Goldsmith Conference,* Toulouse, pp. 971–972. London Minerological Society.

Melekestsev I. V., Braitseva O. A., Erlich E. N., and Kozhemyaka N. N. (1974) Volcanic mountains and plains (in Russian). In *Kamchatka, Kurile and Commander Islands* (ed. I. V. Luchitsky), pp. 162–234. Nauka.

Melekestsev I. V., Braitseva O. A., Sulerzhitsky and L. D. (1988) Catastrophic explosive volcanic eruptions in Kamchatka and the Kurile islands in late Pleistocene-Early Holocene time. *Trans. (Doklady) Acad. Sci. USSR* **301,** 55–59.

Muehlenbachs K. and Byerly G. (1982) ^{18}O enrichment of silicic magmas caused by crystal fractionation at the Galapagos spreading center. *Contrib. Mineral. Petrol.* **79,** 76–79.

Muehlenbachs K., Anderson A. T., and Sigvaldsson G. E. (1974) Low-$\delta^{18}O$ basalts from Iceland. *Geochim. Cosmochim. Acta* **38,** 577–588.

Nakada M. and Yokose H. (1992) Ice age as a trigger of active Quaternary volcanism and tectonism. *Tectonophysics* **212,** 321–329.

Nokleberg W. J., Parfenov L. M., Monger J. W. H., et al. (1998) Phanerozoic tectonic evolution of the circum-north Pacific. Open File Report 98-754. U.S. Geological Survey.

Palin J. M., Epstein S., and Stolper E. M. (1996) Oxygen isotope partitioning between rhyolitic glass/melt and CO_2: An experimental study at 550–950°C and 1 bar. *Geochim. Cosmochim. Acta* **60,** 1963–1973.

Pineau F., Semet M. P., Grassioneau N., Okrugin V. M., and Javoy M. (1999) The genesis of the stable isotope (O, H) record in arc magmas: The Kamchatka's case. *Chem. Geol.* **135,** 93–124.

Plank T. and Langmuir C. H. (1998) The geochemical composition of subducting sediment and its consequences for the crust and mantle. *Chem. Geol.* **145,** 325–394.

Pokrovsky B. G. (2001) *Crustal Contamination of Mantle Magmas by Methods of Isotope Geochemistry* (in Russian). Nauka.

Pokrovsky B. G. and Volynets O. N. (1999) Oxygen-isotope geochemistry in volcanic rocks of the Kurile-Kamchatka arc. *Petrology* **7,** 227–251.

Ponomareva VV., Melekestsev I. V., Kyle P. R., Rinkleff P. G., Dirksen O. V., Sulerzhitsky L. D., Zaretskaia N. E. and Rourke R. (2004) The 7600 (^{14}C) year BP Kurile Lake caldera eruption, Kamchatka, Russia: Stratigraphy and field relationships. *J. Volcanol. Geotherm. Res.*, in press.

Presnall D. C., Dixon T. H., O'Donell T. H., and Dixon S. A. (1979) Generation of mid-ocean ridge tholeiites. *J. Petrol.* **20,** 3–35.

Prueher L. M. and Rea D. K. (2001a) Tephrochronology of the Kamchatka-Kurile and Aleutian arcs: Evidence for volcanic episodicity. *J. Volcanol. Geotherm. Res.* **106,** 67–84.

Prueher L. M. and Rea D. K. (2001b) Volcanic triggering of late Pliocene glaciation: Evidence from the flux of volcanic glass and ice-rafted debris to the North Pacific Ocean. *Palaegeogr. Palaeoclimatol. Palaeoecol.* **173,** 215–230.

Rapp R. P. and Watson E. B. (1995) Dehydration melting of metabasalts at 8–32 kbars: Implications for continental growth and crust-mantle recycling. *J. Petrol.* **36,** 891–931.

Rinkleff P. G. (1999) Petrologic evolution and stratigraphy of the eruptive products from the 7.7ka (^{14}C) Kurile Lake caldera eruption, southern Kamchatka, Russia. M.S. thesis. New Mexico Institute of Mining and Technology.

Rumble D. and Yui T. F. (1998) The Qinglongshan oxygen and hydrogen isotope anomaly near Donghai in Jiangsu Province, China. *Geochim. Cosmochim. Acta* **62,** 3307–3321.

Ryan J. G., Morris J., Tera F., Leeman W. P., and Tsvetkov A. A. (1995) Cross-arc geochemical variations in the Kurile arc as a function of slab depth. *Science* **270,** 625–627.

Savoskul O. S. (1999) Holocene glacier advances in the headwaters of Sredniaya Avacha, Kamchatka, Russia. *Quat. Res.* **52,** 14–26.

Sheppard S. M. F. and Harris C. (1985) Hydrogen and oxygen isotope geochemistry of Ascension Island lavas and granites: Variation with crystal crystallization and interaction with sea water. *Contrib. Mineral. Petrol.* **91,** 74–81.

Sheymovich V. S. (1979) *Ignimbrites of Kamchatka*. Nedra.

Simkin T. and Siebert L. (1994) *Volcanoes of the World*. 2nd ed. Geoscience Press.

Singer B. S., O'Neil J. R., and Brophy J. G. (1992) Oxygen isotope constraints on the petrogenesis of Aleutian arc magmas. *Geology* **20,** 367–370.

Spera F. J. and Bohrson W. (2001) Energy-constrained open-system magmatic processes I: General model and energy constrained assimilation-fractional crystallization (EC-AFC) formulation. *J. Petrol.* **42,** 999–1118.

Stolper E. and Epstein S. (1991) An experimental study of oxygen isotope partitioning between silica glass and CO_2 vapor. Special Publication 3, pp. 35–51. Geochemical Society.

Taran Yu. A., Pokrovsky B. G., and Volynets O. N. (1997) Hydrogen isotopes in amphiboles and micas from Quaternary volcanic rocks of Kurile-Kamchatka arc system. *Geochem. J.* **34,** 203–221.

Taran Yu. A., Pokrovsky B. G., and Glavatskikh S. F. (1988) Isotope data on hydrothermal transformation of rocks in the Mutnovsky geothermal system, Kamchatka. *Geochem. Int.* **25,** 1569–1579.

Tatsumi Y., Kogiso T., and Nohda S. (1995) Formation of a third volcanic chain in Kamchatka: Generation of unusual subduction-related magmas. *Contrib. Mineral. Petrol.* **120,** 117–128.

Taylor H. P. Jr. (1968) Oxygen isotope geochemistry of igneous rocks. *Contrib. Mineral. Petrol.* **19,** 1–71.

Taylor H. P. Jr. and Sheppard S. M. F. (1986) Igneous rocks: I. Processes of isotopic fractionation and isotopic systematics. *Rev. Mineral.* **16,** 227–272.

Tera F., Morris J. D., Leeman W. P., and Tsvetkov A. A. (1990) Further evidence from Be-B systematics for the homogeneity of the subducted component in arc magmatism: Case of the Kurile-Kamchatka arc. *Geochronol. Isotope Geol.* **27,** 100.

Thirlwall M. F., Graham A. M., Arculus R. J., Harmon R. S., and Macpherson C. G. (1996) Resolution of the effects of crustal assimilation, sediment subduction, and fluid transport in island arc magmas: Pb-Sr-Nd-O isotope geochemistry of Grenada, Lesser Antilles. *Geochim. Cosmochim. Acta* **60,** 4785–4810.

Turner S., McDermott F., Hawkesworth C., and Kepezhinskas P. (1998) A U-series study of lavas from Kamchatka and the Aleutians: Constraints on source composition and melting processes. *Contrib. Mineral. Petrol.* **133,** 217–234.

Valley J. W., Kitchen N., Kohn M. J., Niendorf C. R., and Spicuzza M. J. (1995) UWG-2, a garnet standard for oxygen isotope ratio: Strategies for high precision and accuracy with laser heating. *Geochim. Cosmochim. Acta* **59,** 5223–5231.

Vinogradov V. I. (1995) Isotopic evidence of the conversion of oceanic crust to continental crust in the continent-ocean transition zone of Kamchatka. *Geochem. Int.* **32,** 70–109.

Vinogradov V. I. and Vakin Y. A. (1983) Strontium isotopes of the thermal waters of Kamchatka. *Trans. (Doklady) Acad. Sci. USSR* **273,** 965–968.

Volynets O. N. (1994) Geochemical types, petrology and genesis of Late Cenozoic volcanic rocks from the Kurile-Kamchatka island-arc system. *Int. Geol. Rev* **36/4,** 373–405.

Volynets O. N., Ponomareva V. V., Braitseva O. A., Melekestsev I. V., and Chen C. H. (1999) Holocene eruptive history of Ksudach volcanic massif, South Kamchatka: Evolution of a large magmatic chamber. *J. Volcanol. Geotherm. Res.* **91,** 23–42.

Volynets O. N., Babanskii A. D., and Gol'tsman Y. V. (2000) Variations in isotopic and trace elemental composition of lavas from volcanoes of the Northern group, Kamchatka, in relation to specific features of subduction. *Geochem. Int.* **38,** 974–989.

Vroon P. Z., Lowry D., Van Bergen M. J., Boyce A. J., and Mattey D. P. (2001) Oxygen isotope systematics of the Banda Arc: Low-δ^{18}O despite involvement of subducted continental material in magma genesis. *Geochim. Cosmochim. Acta* **65,** 589–609.

Widom E., Kepezhinskas P., and Defant M. (2003) The nature of metasomatism in the sub-arc mantle wedge: Evidence from Re-Os isotopes in Kamchatka peridotite xenoliths. *Chem. Geol.* **196,** 283–306.

Yogodzinski G. M., Lees J. M., Churikova T. G., Dorendorf F., Woerner G., and Volynets O. N. (2001) Geochemical evidence for the melting of subducting oceanic lithosphere at plate edges. *Nature* **409,** 500–504.

Zhao Z.-F. and Zheng Y.-F. (2003) Calculation of oxygen isotope fractionation in magmatic rocks. *Chem. Geol.* **193,** 59–80.

Zhuravlev D. Z., Tsvetkov A. A., Zhuravlev A. Z., Gladkov N. G., and Chernyshev I. V. (1987) ^{143}Nd/^{144}Nd and ^{87}Sr/^{86}Sr ratios in recent magmatic rocks of the Kurile island arc. *Chem. Geol.* **66,** 227–243.

Zielinski G. A., Mayewski Meeker L. D., Whitlow S., and Twickler M. (1996) A 110 000-year record of explosive volcanism from the GISP2 (Greenland) ice core. *Quat. Res.* **45,** 109–118.

Zolotarev B. P., Karpov G. A., Yeroshev-Shak V. A., Artamonov A. V., Grigoryev V. S., and Pokrovsky B. G. (1999) Evolution of volcanism in Uzon caldera. *Volcanol. Seismol.* **6,** 67–84.